

# **Pixel Classification Algorithms for Noise Removal and Signal Preservation in Low Pass Filtering**

Sha Gong

A Thesis  
in  
The Department  
of  
Electrical and Computer Engineering

Presented in Partial Fulfillment of the Requirements  
for the Degree of Master of Applied Science (Electrical and Computer Engineering) at  
Concordia University  
Montreal, Quebec, Canada

December, 2013  
© Sha Gong, 2013

**CONCORDIA UNIVERSITY  
SCHOOL OF GRADUATE STUDIES**

This is to certify that the thesis prepared

By:           Sha Gong

Entitled:    “Pixel classification algorithms for noise removal and signal preservation in  
                  low pass filtering”

and submitted in partial fulfillment of the requirements for the degree of

**Master of Applied Science**

Complies with the regulations of this University and meets the accepted standards with respect to originality and quality.

Signed by the final examining committee:

_____	Chair
Dr. M. Z. Kabir	
_____	Examiner, External
Dr. Y. Zeng (CIISE)	To the Program
_____	Examiner
Dr. M. O. Ahmad	
_____	Supervisor
Dr. C. Wang	

Approved by: \_\_\_\_\_  
  Dr. W. E. Lynch, Chair  
  Department of Electrical and Computer Engineering

\_\_\_\_\_ 20 \_\_\_\_\_

\_\_\_\_\_

Dr. C. W. Trueman  
Interim Dean, Faculty of Engineering  
and Computer Science

# **Abstract**

## **Pixel Classification algorithms for noise removal and signal preservation in low pass filtering**

**Sha Gong**

Contrast enhancement is essential to improve the image quality in most of image pre-processing. A histogram equalization process can be used to achieve a high contrast. It causes, however, also noise generation. Involving a low-pass filtering process is an effective way to achieve a high-quality contrast enhancement with low-noise, but it leads to the conflict between noise removal and signal preservation. To perform discriminative low-pass filtering operations with the presence of noises and signal variations in different regions, it is thus necessary to develop good algorithms to classify the pixels.

In this thesis, two classification algorithms are proposed. They aim at low-contrast images where gradient signals are severely degraded by various causes during the acquisition process. They are to classify the pixels according to the initial gray-level homogeneity of their regions. The basic classification method is done by gradient thresholding, and the threshold values are generated by means of gradient distribution analysis. To tackle the problems of various gradient degradation patterns in low-contrast images, image pixels are grouped in a particular way that, in the same group, pixels in

homogeneous regions can be easily distinguished from those in non-homogeneous regions by the basic method of simple gradient thresholding. Two algorithms based on different grouping methods are proposed. The first algorithm aims at high dynamic range images. The pixels are first grouped according to their gray-level ranges, as the gradient degradation is, in such a case, gray-level-dependent. The gradient distribution of each sub-range is obtained and a pixel classification is then made to adapt to their original gray-level signals in the sub-range. The other algorithm is to tackle a wider range of low-contrast images. In this algorithm, a gray-level histogram thresholding is performed to divide the pixels into two groups according to their likelihood to homogeneous, or non-homogeneous, pixels. Thus, in one group a majority of homogeneous pixels is established and in the other group the majority is of non-homogeneous pixels. The classification done in each group is to identify those in the minority.

Both proposed algorithms are very simple in computation and each of them is incorporated into the contrast enhancement procedure to make the integrated low-pass filters effectively remove the noise generated in the histogram equalization while well preserving the signal details. The simulation results demonstrates, by subjective observation and objective measurements, that the proposed algorithms lead to a superior quality of the contrast enhancement for varieties of images, with respect to two advanced enhancement schemes.

# Acknowledgement

First, I would like to take this opportunity to express my sincere gratitude to my supervisor Prof. Chunyan Wang for all I have learned from her and her continuous help in all stages of this thesis. I want to thank her for her immense support and valuable guidance for encouraging and helping me to shape my interest and ideas. She has always been a strong and supportive adviser to me throughout my graduate school career.

I also want to acknowledge my colleagues for their selfless help and advice during my research. Their kindness and patience give me a strong support and comfort at the beginning of my research.

Finally, I want to give my deepest appreciation to my family for their continuous love and supports in my decisions, especially my boyfriend who always believes in me and stands on my side whenever I feel struggling and frustrated. Without them I could not have made this happen.

## Table of Content

List of Figures.....	viii
List of Tables.....	x
List of Acronyms and Abbreviations.....	xi
List of Symbols.....	xii
List of Terminology.....	xiii
Chapter 1. Introduction.....	1
1.1. Subject of the work.....	1
1.2. Challenges in the design of pixel classification algorithms.....	2
1.3. Motivation and objective.....	4
1.4. Scope and organization of the thesis.....	5
Chapter 2. Background and Relevant Work.....	7
2.1. Introduction.....	7
2.2. Fundamentals of contrast enhancement.....	8
2.2.1. Histogram Equalization.....	8
2.2.2. Low-pass filters.....	10
2.2.3. High-pass filters used to detect gray-level variations.....	11
2.3. Relevant work.....	13
2.3.1. Advanced histogram equalization.....	13
2.3.2. Filters in the contrast enhancement.....	15
2.3.3. Existing classification methods.....	19
2.4. Summary.....	24
Chapter 3. Description of Proposed Algorithm.....	25
3.1. Overview.....	25
3.2. Analysis of the gradient distribution and the threshold generation for pixel classifications.....	27
3.3. Classification algorithm with pixel grouping based on gray level ranges.....	34

3.4.	Classification algorithm with pixel grouping by histogram-thresholding.....	41
3.5.	Summary.....	50
Chapter 4.	Simulation Results and Evaluations.....	52
4.1.	Introduction.....	52
4.2.	Simulation conditions.....	52
4.3.	Simulation results.....	54
4.4.	Summary.....	62
Chapter 5.	Conclusion.....	64
5.1.	Concluding remarks.....	64
5.2.	Future work.....	67
References	.....	68
Appendix	.....	73
	Values of the parameters used in the simulation of TMR filtering method [3].....	73
	Values of the parameter used in the simulation of adaptive clipping method [4].....	73

## List of Figures

Figure 1.1. Block diagram of contrast enhancement involving LP filters.....	1
Figure 1.2. Response of real films, digital cameras to the irradiance. The y-axis represents the normalized brightness of the image [2].....	3
Figure 2.1. Kernels of SOBEL operators emphasizing variations on different directions.....	11
Figure 2.2. Filter structure proposed in [32].....	14
Figure 2.3. Iterated TMR filtering of contrast enhanced image.....	15
Figure 2.4. Block diagram of contrast enhancement involving multi-stage LP filters.....	16
Figure 2.5. (a) The distribution of regional gradient means. The first “dip” point in the curve denotes the initial gradient threshold. (b) An example of misclassification [38].....	18
Figure 2.6. Pixel classification with region correction.....	20
Figure 3.1. Schematic diagram of the proposed algorithm.....	23
Figure 3.2. (a) Test image. (b) Gradient map of image (a).....	24
Figure 3.3. (a) Gradient distribution obtained from the gradient map shown in Figure 3.2(b). The y-axis is the normalized value of the distribution, and $G_r$ of x-axis is the SOBEL-weighted gradient value, i.e., the height of the gradient bin. (b) First derivative of the outline curve presented in (a). (c) Second derivative of the outline curve presented in (a).....	26
Figure 3.4. Procedure to define the three gradient values $Th_L$ , $Th_M$ , $Th_H$ used in the gradient-based classification.....	28
Figure 3.5. (a) Test image. (b) Mask generated by thresholding the gradient map of the image shown in (a) with the threshold $Th_H = 38.8$ . (c) Mask generated by thresholding the gradient map of the image shown in (a) with the threshold $Th_M = 17.1$ . (d) Mask generated by thresholding the gradient map of the image shown in (a) with the threshold $Th_L = 14.9$ .....	28
Figure 3.6. (a) An HDR test image. (b) Gradient distribution obtained from the gradient map of the image shown in (a).....	31
Figure 3.7. Process of mask generation.....	32
Figure 3.8. Block diagram of the algorithm for the pixel classification.....	33
Figure 3.9. Block diagram of the classification shown in Figure 3.8.....	33
Figure 3.10. Block diagram of the combination shown in Figure 3.8.....	34
Figure 3.11. (a) Gradient distribution of the entire image displayed with the distributions of the three sub-images. (b) Local gradient distribution and its 1st order derivative for the pixels ranged from 0 to 100. (c) Local gradient distribution and its 1st order derivative for the pixels ranged from 101 to 200. (d) Local gradient distribution and its 1st order derivative for the pixels ranged from 201 to 255.....	35

Figure 3.12. Masks obtained by threshold generation. (a) Mask corresponding to gradient level $Th_L$ . (b) Mask corresponding to gradient level $Th_M$ . (c) Mask corresponding to gradient level $Th_H$ .....	36
Figure 3.13. Low-contrast images and their histograms. (a1) (a2) X-ray. (b1) (b2) Window and Desk. (c1) (c2) Pollen Grain.....	38
Figure 3.14. Histogram thresholding of an image to group the pixels. The binary mask $B$ indicates the positions of the pixels in the undashed bins with Logic-1 status and the others Logic-0.....	39
Figure 3.15. Block diagram of Algorithm 2.....	42
Figure 3.16. Detailed block diagram of the pixel grouping and the classification in the diagram shown in Figure 3.15.....	42
Figure 3.17. Example of the gradient distribution of a pixel group.....	43
Figure 3.18. (a) Histogram of the test image shown in Figure 3.6(a). (b) Gradient distributions of $I_g$ . The solid curve is given by the pixels of the entire $I_g$ . When the pixels are grouped with $T_{G2}$ , which is 30% of the maximum height, the low-bin group yields the dashed curve and high-bin group the dot-dashed one.....	44
Figure 3.19. Binary masks obtained by applying the algorithm 2. They can be used in the procedure shown in Figure 3.15. (a) <i>Mask 1</i> . (b) <i>Mask2</i> . (c) <i>Mask 3</i> .....	45
Figure 4.1. (a) Original image of X-ray. (b) By CLAHE. (c) By CLAHE combined with the iterated TMR filters. (d) By the adaptive clipping method. (e) By the procedure involving the proposed algorithm 1. (f) By the procedure involving the proposed algorithm 2.....	51
Figure 4.2. (a) Original image of Pollen Grain. (b) By CLAHE. (c) By CLAHE combined with the iterated TMR filters. (d) By the adaptive clipping method. (e) By the procedure involving the proposed algorithm 1. (f) By the procedure involving the proposed algorithm 2.....	53
Figure 4.3. (a) Original image of Window and Desk. (b) By CLAHE. (c) By CLAHE combined with the iterated TMR filters. (d) By the adaptive clipping method. (e) By the procedure involving the proposed algorithm 1. (f) By the procedure involving the proposed algorithm 2.....	55

## List of Tables

Table 3.1: Gradient based classification.....	25
Table 3.2: Threshold values for pixel classification.....	36
Table 3.3.....	41
Table 4.1: PSNR of the iterated TMR filtering, adaptive clipping and the two proposed algorithms.....	56
Table 4.2: PFOM of the iterated TMR filtering, adaptive clipping and the two proposed algorithms.....	56
Table 4.3: Average elapsed time in second.....	57

## **List of Acronyms and Abbreviations**

HE	Histogram Equalization
AHE	Adaptive Histogram Equalization
CLAHE	Contrast Limited Adaptive Histogram Equalization
HDR	High Dynamic Range
LP	Low-Pass
HP	High-pass
TMR	Transportation Map Regularization
PFOM	Pratt's Figure of Merit
PSNR	Peak Signal to Noise Ratio

## List of Symbols

$I(i,j)$	Input image
$I_g(i,j)$	Gradient map of the input image
$I_c(i,j)$	Contrast enhanced image
$B(i,j)$	Binary mask for LP filtering
$I_{out}(i,j)$	Output image
$G_L$	Gray level value
$H(G_L)$	Gray level histogram of an image
$G_r$	Gradient value
$H(G_r)$	Gradient histogram of an image
$g_r(i,j)$	Gradient signal
$Th_L$	Gradient value at $G_r = Th_L$ , $\left  \frac{dH(G_r)}{d(G_r)} \right _{\max}$ and $\frac{d^2H(G_r)}{d^2G_r} = 0$ .
$Th_M$	Gradient value at $G_r = Th_M$ , $\frac{d^2H(G_r)}{d^2G_r}_{\max}$
$Th_H$	Gradient value at $G_r = Th_H$ , $\left  \frac{dH(G_r)}{dG_r} \right  \approx 0$
$T_G$	Gray-level histogram threshold
$\sigma$	Standard deviation of Gaussian filter

## **List of Terminology**

Homogeneous pixels

Pixels located in homogeneous regions.

Non-homogeneous pixels

Pixels located in non-homogeneous regions.

# Chapter 1. Introduction

## 1.1. Subject of the work

Contrast enhancement is one of the basic operations in image processing. One commonly employed method to achieve a good contrast is histogram equalization (HE). In particular, adaptive histogram equalization (AHE) processes are developed to enhance the contrast of image details. However, while the pixel signal is enhanced, the noise is also amplified. Therefore, a lot of research work has been done to solve the conflict between detail enhancement and noise generation during a histogram equalization process. Varieties of advanced AHE attempt to minimize the noise by means of modulating transformation functions. Such a noise removal method has its limitation of achieving both good contrast enhancement and effective noise removal. Therefore, it has been proposed to have low-pass (LP) filters placed after HE to obtain high-quality low-noise images [1]. The basic block diagram of the contrast enhancement involving LP filters is shown in Figure 1.1.

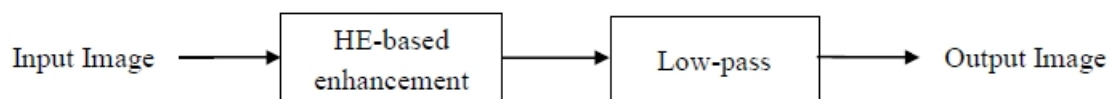


Figure 1.1. Block diagram of contrast enhancement involving LP filters.

The involvement of low-pass filtering allows the enhancement of the image contrast and the reduction of the noise to be performed separately to gain a good contrast with a low level of noise. A critical issue in the design of the LP filters is the conflict between

noise removal and signal preservation, as the smoothing operations performed by LP filters may erase both noise and signal variations. Hence, the filtering must be discriminative to protect signal variations from being erased. To this end, varieties of local-signal-dependent LP filtering methods have been proposed. To implement the signal dependency, one can use local information to modulate the parameters in the function of a LP filter, which may lead to a complex filter structure. One can also use simple LP filters to perform smoothing operations and masks to expose/protect the pixels in the operations. In this case, the pixels need to be classified based on certain criteria, such as gray level homogeneity, to generate the controlling masks. The quality of the LP filtering is closely related to that of the classification. The work presented in this thesis is in the aspect of the pixel classification to improve the quality of the low pass filtering operations in order to remove the noise generated in the contrast enhancement.

In this chapter, the problem and challenge in the design of the classification algorithms is addressed in Section 1.2. The motivations and the objective of the work are stated in Section 1.3. The scope of the work and the organization of the thesis are described in Section 1.4.

## ***1.2. Challenges in the design of pixel classification algorithms***

As described above, the application of low-pass filters can be a solution to the

conflict between contrast enhancement and noise removal since these two issues can be dealt with separately. However, the LP filtering operations may erase the signal variations while removing the noise, introducing another conflict between signal preservation and noise removal. In order to perform the smoothing operations selectively, it is necessary to classify the pixels according to the homogeneity of their regions.

The homogeneity of gray levels in a region is related to the gradients of pixel signals. A gradient detection is involved in most of the pixel classification methods. However, the degree of the homogeneity is not simply proportional to the gradients. In most cases, the gradient signals of low-contrast images are degraded by various causes. Acquiring high-dynamic-range (HDR) images by a medium-range camera can cause gradient compression, due to nonlinear transformation functions, as shown in Figure 1.2, of the acquisition devices. It is often the case that the compression in the higher ranges is very different from that in the lower ones.

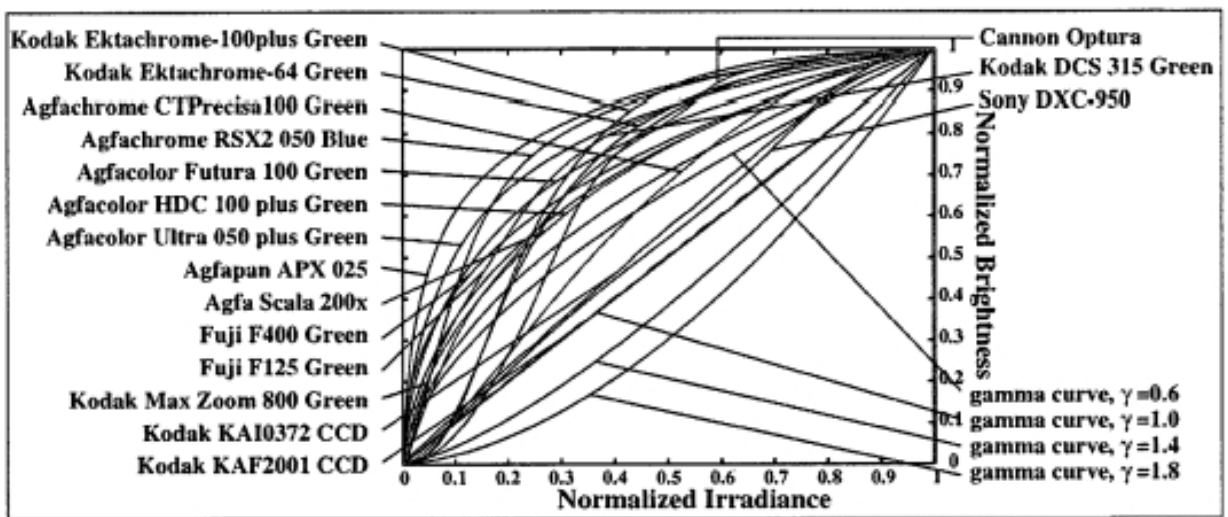


Figure 1.2. Response of real films, digital cameras to the irradiance. The y-axis represents the normalized brightness of the image [2].

The gradient degradation can be in different forms. Images acquired from long distances may not have problems caused by over-and-under exposure that occurs in case of HDR images, but their gradient signal attenuation can be very severe and the signal detection is very delicate to handle. Medical images can also have the problems of low contrast, mostly due to, low-level intensity of projection in imaging. The signal variations are reflected poorly in the acquired images. This imaging process results in complex patterns of gradient degradations making the gradient-based signal detection and classification a challenging task.

The processing time for the pixel classification with respect to that of the other blocks in the system is another important concern in the design. The processing time for the classification should be short enough so that the low-pass filters do not need to wait long time for the completion of the classification after CLAHE is finished. Considering the complexity of the gradient degradation, we need to develop signal-dependent classification algorithms addressing different problems in the images, which often lead to a time-consuming computation process. It is thus another challenge to make the algorithm simple and effective.

### ***1.3. Motivation and objective***

Image pre-processing is to obtain low-noise high-contrast images from poor-quality input ones. High contrast can be obtained by HE but low-noise is not easy to achieve.

However, as the quality of the pre-process images can have an effect on that of the succeeding image signal extractions, high-quality noise removal is essential. In the contrast enhancement scheme shown in Figure 1.1, this high-quality depends on how the LP operations can be performed to the noise part of the pixel gray level and preserve the signal part. To this end, a good classification is essential.

The objective of the work presented in this thesis is to develop simple algorithms of the pixel classification according to the homogeneity of gray levels. Its result will be used to generate masks to implement discriminative low-pass filtering operations in the contrast enhancement scheme for noise removal and signal preservation to achieve a high-quality low-noise enhancement. Controlling masks provide the low-pass filtering operations with different levels of exposure/protection so that different pixel groups to effectively remove the noise while signal variations are protected can be given different levels of smoothing operations.

#### ***1.4. Scope and organization of the thesis***

The work presented in this thesis is to develop algorithms to classify the pixels in low-contrast images in which the signal quality may be severely affected by gradient degradation. In order to achieve satisfactory classification results, characters of gradients of different pixel groups will be analyzed. The relationship among the gray level homogeneity in the image, gray level distribution and signal gradients will be studied.

The work will be focused on developing algorithms in which the image pixels are grouped in such a way that a simple gradient-based classification method can be applied to achieve high-quality pixel classification.

The thesis is organized as follows. In chapter 2, basic image processing building blocks used in this work are briefly described and some existing methods for the classification and contrast enhancement relevant to the work are presented. Two algorithms of the pixel classification are proposed in chapter 3. A performance evaluation of the contrast enhancement involving the proposed algorithms is presented in chapter 4. The results have been examined by subjective observation and objective measurements, and compared with those resulting from two contrast enhancement algorithms reported recently. The work of the thesis is concluded in chapter 5.

# Chapter 2. Background and Relevant Work

## *2.1. Introduction*

In real world, due to the limitation of illumination conditions and acquisition devices, image quality can be degraded in various ways causing information to be shaded. Therefore, as being capable of enhancing detailed information in images, contrast enhancement became a fundamental necessity in most image processing applications.

A variety of methods to improve image contrast have been developed, including histogram equalization (HE) and gray level stretching [3] [4], among which HE is generally preferred because of its effectiveness and simplicity. Intensive researches have been investigated trying to remove the noise generated in HE. Some of the approaches, e.g., [5], are based on the modulation of the transformation function in order to make it adaptive to input signals. Another method to overcome the limitation of HE is using LP filters after HE. However, in order to avoid the attenuation of the original signals, the low-pass filters need to be made discriminative according to the signal density and noise severity in different regions of the image, such as the detail-preserving filters in [6] and ideal masks in [7]. The challenge of this method is the classification of pixels in order to determine which regions should be protected and the strength of the low-pass filters for different noisy regions.

In this chapter, an introduction of some fundamental conceptions in contrast enhancement is given in Section 2.2. Some recent progress on improving the performance

of contrast enhancement is reviewed in Section 2.3. A brief summary is presented in Section 2.4.

## ***2.2. Fundamentals of contrast enhancement***

### ***2.2.1. Histogram Equalization***

Generally, there are two kinds of histogram equalization, global HE [8] [9] and adaptive HE [10]. The global HE is the standard method and the adaptive HE is a variation of the global HE.

Standard HE process enhances the contrast of an image by uniformly distributing all pixels along all the gray levels in the histogram, which gives the entire image a maximum dynamic range. The gray level transfer function for general HE can be expressed as

$$h(v) = \text{round}\left(\frac{cdf(v) - cdf_{\min}}{(M \times N) - cdf_{\min}} \times (L - 1)\right),$$

where  $cdf_{\min}$  is the minimum non-zero value of the cumulative distribution function,  $M \times N$  gives the dimensions of the image and  $L$  is the number of grey levels.

Through such a transformation process, the dynamic range of the image is stretched to  $(L-1)$ . However, if the input image already has a high dynamic range (HDR), i.e., some regions of the image are significantly lighter or darker than the other parts, the effect of a global HE will be greatly weakened.

This limitation in global HE can be overcome by adaptive histogram equalization (AHE). In this method, the image is divided into a number of tiles and the histograms for

each tile are generated to derive a unique transfer function for the local HE. Therefore, even for an HDR image, it is still capable to improve the local contrast and bring out more local details. However, even though AHE is more powerful in stretching the local contrast, it introduces the speckle noise in a region where the majority pixels are homogeneous ones. In such regions, most local pixels have very similar gray levels, which form a high peak in the local histogram. This high peak then leads to a high slope in its CDF function causing the transfer function to be very sensitive to the gray levels around these peaks in the histogram. Eventually, small variations in a relatively flat region are amplified and this region becomes a less flat region with many speckle noises.

To avoid such a drawback of AHE, a variation of AHE emerges, which is known as contrast limited adaptive histogram equalization (CLAHE) [11]. Differing from ordinary HE method, CLAHE limits the local contrast enhancement by clipping the bins in the histogram that are higher than a global limit before computing the CDF. As discussed before, high peaks in the histogram means a high slope in its CDF, therefore, by clipping the pixels in those peaks and evenly redistributing them into every bin, one can reduce the slope and hence alleviate the gray level stretching around those peaks.

In most applications, CLAHE is usually used as a trade-off between the local contrast and the amount of the speckle noises in the output image, such as fog removal presented in [12]. But meanwhile its contrast performance will be attenuated. Therefore, in order to achieve an optimum local contrast without introducing more noises, a denoising process using low-pass filter after CLAHE is required.

### 2.2.2. *Low-pass filters*

In view of the fact that traditional HE introduces speckle noises, one needs a denoising process to suppress these noises while maintaining the original signal variations. Many kinds of LP filters are designed for various purposes or demands for noise removal, such as Gaussian filters [13], mean-based filters [14], median-based filters [15], bilateral filters [16] and Yaroslavsky neighborhood filters [17]. Among these filters, the first three are commonly used because of their relatively low computation intensity and good performance.

Gaussian blur is one of the most fundamental ways to smooth the image by replacing the center pixel with the weighted average of neighboring pixels. A two-dimensional Gaussian function is defined as

$$g(x, y) = \frac{1}{2\pi\sigma^2} e^{-\frac{x^2+y^2}{2\sigma^2}},$$

where  $\sigma$  is the standard deviation, which is typically used to adjust the “strength” of its smoothing effect. Its simplicity and effectiveness in the suppression of the random noise make it a preference for noise removal. Mean-based filters can be seen as a special case of Gaussian filter.

Another example of smoothing filters is median-based filters. Unlike the average/mean filters, it replaces the existing value with one of those present in its neighborhood. It will not be affected if one of its neighboring pixels is much larger or smaller than the others. Thus, it can provide a good image quality in terms of preserving

signal variations during the smoothing process. Moreover, as the median filter does not introduce any new gray levels, it can be applied repeatedly to strengthen the noise smoothing effect. However, this filter cannot preserve the corners of the image objects and may erase very thin lines.

One can choose a certain type of LP filters according to its design requirements. However, no matter which kind of LP filter one chooses, there still exists the problem of signal attenuation or loss during the smoothing process. Therefore, it is essential to develop an effective classification method to generate controlling masks for different levels of protection/exposure during LP filtering operations.

### ***2.2.3. High-pass filters used to detect gray-level variations***

For the sake of not impairing any useful signals during noise removal, all signals should be extracted and protected in advance. In order to achieve such goal, one needs to have the knowledge of the characteristics of both noises and signals.

The pixels representing a particular feature (e.g. edges/textures, flat regions) of the image usually have a common distribution of gray level variations. Therefore, by inspecting the distributions of the gray level variations, the pixels can be classified into different regions, such as, objective edges, textures and flat regions. In the practical applications, the pixel classes can be more specific, such as stars and background in astronomy pictures or human faces in a face recognition system. General pixel classifications have already been used in a wide range of image systems, such as camera

system, traffic control systems, agricultural imaging, computer vision and etc [18]. Commonly used approaches for gray scale image classification include histogram based approach [19], clustering approach [20], watersheds transformation approach [21], classifier method and neural networks.

A fundamental application of pixel classification is to split objective edges and other flat areas in the image, namely, edge detection. A basic way to achieve this is by applying a proper threshold which is obtained by inspecting the pixel population on the histogram [22]. However, such kind of classification only works when the edges and flat regions are clearly distinguishable in gray level, which is very rare for the real images. For many images with high dynamic range (HDR), both homogeneous and non-homogeneous pixels are randomly distributed in almost all gray levels. In this case, the classification simply by inspecting the histogram is not sufficient and a further correction of the misclassified pixels is required. As the nature of the edges is some sharp changes in gray level, we need another metric which can indicate the gray level variations for edge detection. Then by applying a proper threshold on this metric, one can extract the edges in the image.

High pass filters are used to be an option for the extraction of edges. So far, many kinds of edge enhancement operators are developed. These operators are based on convolving the image with a small, separable, and integer-valued filter and therefore reducing computations. Examples include PREWITT, SOBEL and LAPLACIAN

operators, all of which can indicate the extent of gray level variations by simply doing a convolution with the input image.

However, as any single operator can only indicate gray level variations in a single direction, it is of more accuracy to combine multiple operators and calculate the gray level gradient vector [23]. The kernels of SOBEL operator, detecting the gray level variation in the horizontal, vertical and diagonal directions, used in this thesis is shown in Figure 2.1.

1	0	-1	1	2	1	0	1	2	2	1	0
2	0	-2	0	0	0	-1	0	1	1	0	-1
1	0	-1	-1	-2	-1	-2	-1	0	0	-1	-2

Figure 2.1. Kernels of SOBEL operators emphasizing variations on different directions.

Once one has such a “gradient map” indicating how the gray level varies all over the image, edges can be determined by applying a threshold on the gradient or any other similar metrics. Multiple approaches have been proposed to find the optimum thresholding way for precise classifications [24].

## ***2.3. Relevant work***

### ***2.3.1. Advanced histogram equalization***

Many variations based on the original histogram equalization have been investigated in order to improve their performance of contrast enhancement. Most of them fall into

two categories, the first of which is to make the transformation function of histogram equalization more adaptive to local image signals. It can be done by modulating the “local” cumulative functions [25] or by weighted threshold HE [26].

In [27], a smart contrast enhancement technique based on traditional HE algorithm is proposed. This dynamic histogram equalization (DHE) technique aims at good detail preservation during contrast enhancement. It segments the image histogram according to its local information and assigns specific gray level ranges for each segment before equalizing them separately. This process will be repeated in order to ensure an even distribution.

Some other methods of advanced AHE are based on the modulation of the parameters involved in the mapping function according to its homogeneity, such as CLAHE [28]. However, in the standard CLAHE, a global clip limit will be applied to all tiles, which results in improper histogram clipping in some local regions. Therefore, a new tone mapping algorithm for HDR images has been presented in [29]. In order to alleviate the artifacts introduced by the standard CLAHE algorithm, each contextual region is applied with an individual clip limit defined as

$$\alpha = a \cdot \text{mean}(I_{k,l}(i, j)) + 12(1 - a) \cdot \text{var}(I_{k,l}(i, j)),$$

where  $\alpha$  is the normalized clip limit,  $a$  is a weight factor between  $[0, 1]$ ,  $I_{k,l}(i, j)$  is the pixel gray level on  $i^{\text{th}}$  row and  $j^{\text{th}}$  column and factor  $12$  is used to renormalize the variance value.

Improvements have also been made on the strategy of redistributing the excess pixels over the clip limit. Instead of redistributing them equally to all bins, in this way the excess pixels are put in a “decision bag” [29]. A bin that does not reach the clip limit but with at least one of its two neighbors reaches will be filled with pixels obtained from the bag. In this way, all the pixels are assigned in the neighborhoods of the peaks in the histogram.

The work presented above demonstrates a good visual quality in an automated way without the need to define any external parameter. The local details are improved regardless of the original local intensity. However, no matter how automatic and precise the clip limit is, there still exists the limitation for such method since its noise removal is at a cost of lower contrast enhancement.

### ***2.3.2. Filters in the contrast enhancement***

In order to perform the enhancement of the image contrast and the reduction of the noise separately, another approach involving LP filters is widely used. Many studies have been investigated in this area by introducing extra denoising processes after finishing a contrast enhancement process to remove the speckle noises. A dynamic non-local mean-based filter is introduced in [30] to remove the noise in magnetic resonance images after a dynamic contrast enhancement. Work in [31] aims at developing a good noise removal method specifically for Poisson and Gaussian mixture noise generated during the contrast enhancement process.

In [32], a low-pass filter and a high-pass filter are combined to generate a filter mask for the purpose of signal protection. The filter mask is defined as a class of surrounding pixels with similar signal features to the current pixel. The filter structure is displayed in Figure 2.2. Compared with other quadratic filters [33], this robust nonlinear contrast enhancement filter shows good signal preservation for blurred and noisy images during the process of contrast enhancement.

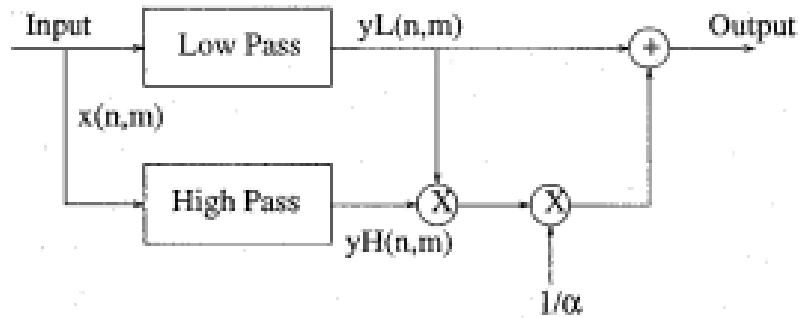


Figure 2.2. Filter structure proposed in [32].

Another example involving LP filters is presented in [34] with a view to removing the blocking effects while maintaining the advantages of AHE with a fine visual quality. Such method is based on partially overlapped sub-block histogram equalization (POSHE). However, in order to completely get rid of the blocking effects, a considerable number of overlapping is needed, which may increase the computation complexity. Moreover, its application in image processing may be limited because of its incapability of scaling for large sub-block and image sizes. Thus, a generalization of the POSHE approach involving cascaded multi-step binomial filtering HE (CMBFHE) [35] is proposed. Compared to the original POSHE method, its performance in scaling for large sub-block sizes and large image sizes is significantly improved with less computational complexity.

In [1], another noise removal method based on transportation map regularization (TMR) filter is proposed. Such TMR filter can be expressed as

$$TMR_u(T(u)) = Y_u(T(u)) + u - Y_u(u),$$

where  $u$  is the original image,  $T(u)$  is the contrast modified image,  $Y_u$  is a non-local operator. The first part of the equation  $Y_u(T(u))$  represented a blurred image due to low-pass filtering, while the second part  $u - Y_u(u)$  is added to restore the image details.

In order to remove all the artifacts, this regularization process should be made iterative and the filtering process can be presented as

$$TMR_u^k(T(u)) = Y_u^k(T(u) - u) + u,$$

where  $Y_u^k$  refers to the recursive use of  $Y_u$  filter.

With a view to controlling the iterations of the TMR filters, a convergence map  $C(x)$  is used and defined as

$$C(x) = \| Y_u^k(T(u) - u) - Y_u^{k-1}(T(u) - u) \|,$$

For a pixel  $x$ , the iteration of the filtering process will be continuous until  $C(x)$  is smaller than a user-defined threshold  $t$  (in many case,  $t=1$ ). The whole procedure of the iterated TMR filtering can be represented by the following scheme [36].

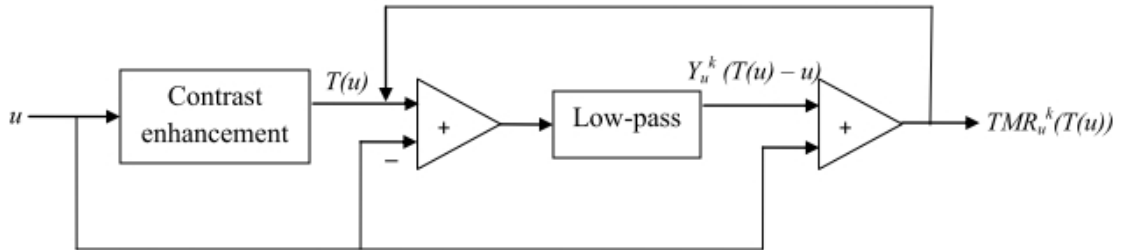


Figure 2.3. Iterated TMR filtering of contrast enhanced image.

As shown in Figure 2.3, the input image is involved both before and after low-pass filtering in every loop. The quality of the output image is, therefore, significantly depended on the quality of the input image, which results in a limitation for its noise removal. Moreover, the involvement of low-pass filters may blur fine details without any protection of the pixel signals. As for the computation, because of the iterations, it is very time-consuming.

One effective way for maintaining the signal variations is to use a series of discriminative LP filters to adjust the degree of smoothing according to the presence of the noise and pixel signals. The scheme shown in Figure 2.4 uses a multi-stage low-pass filtering process to achieve such adaptive noise removal [36].

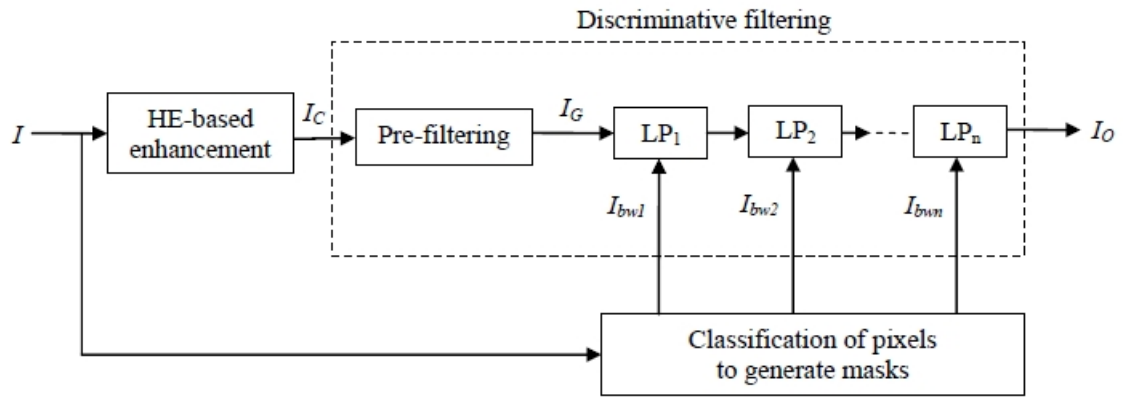


Figure 2.4. Block diagram of contrast enhancement involving multi-stage LP filters.

In order to protect signal variations during the low-pass filtering operations, the regions existing some pixel signals should not be given the same smoothing strength as those flat ones. Therefore, a low-pass filtering is implemented by successive stages of simple low-pass filers. Such multi-stage low-pass filters make the strength of the filtering

progressive, giving different regions different levels of smoothing. The masks controlling each of the low-pass stages make the filtering discriminative. The different coverage by the binary masks allows the multi-stage LP filtering to be applied progressively in different categories of regions with different purpose of protection/exposure. The image quality, therefore, is based on the quality of the controlling masks. Because of its superior performance in both noise removal and contrast enhancement with the protection of signal variations, in this thesis, it is applied as a starting point to be researched.

### ***2.3.3. Existing classification methods***

It is obvious that the usage of post-HE low-pass filters may reduce the effects of the contrast enhancement by degrading its signal variations. Therefore, it necessitates a good classification method to preserve pixel signals and expose noise while applying the LP filters.

As described previously in [29], the parameter  $a$  is used to weight the linear dependence between the mean and the gray level variance. Once the factor  $a$  is determined, the normalized clip limit of CLAHE will be generated automatically, applying to classify the pixels into bright regions and dark regions. Experimentally, it has been observed that for bright regions with high gray levels and high variance, the best normalized clip limit of CLAHE falls into the interval [0.005–0.01], while for dark areas the clip limit should be in the range [0.01 – 0.015]. Based on this observation, an automatic calculation of the adaptive normalized clip limit is used to decide which region

the pixels should belong to, making the classification more adaptive to the local information.

Recently, a denoising technique based on improved adaptive directional lifting wavelet transform (ADL) [37] is proposed in order to separate noise from image signal. Since ADL is normally inaccurate in a noisy image, a classification method based on the pixel pattern is implemented so that ADL can be applied in a noise-free environment. Suppose the noisy in an image is additive zero-mean white Gaussian noise whose variance is  $\sigma_n^2$ , the variance of a local window  $\sigma_{n\_im}^2$  can be represented in different ways. In smooth region,  $\sigma_{n\_im}^2 = \sigma_n^2$ , and in texture region,  $\sigma_{n\_im}^2 = \sigma_{im}^2 + \sigma_n^2$ . Therefore, for each pixel  $Y(i,j)$ ,

$$\begin{aligned} flag_{Y(i,j)} &= 0, & \text{if } \sigma_{Y(i,j)}^2 / \sigma_n^2 \leq T \\ flag_{Y(i,j)} &= 1, & \text{if } \sigma_{Y(i,j)}^2 / \sigma_n^2 > T, \end{aligned}$$

where  $\sigma_{Y(i,j)}^2$  is the variance of the local window centered by the pixel  $Y(i,j)$ ,  $T$  is the threshold defined by researchers. If  $flag_{Y(i,j)} = 0$ , the pixel  $Y(i,j)$  belongs to the smooth region, otherwise it is in the texture region. By applying this pixel classification method, pixel signals can be distinguished from noise, providing a good foundation for the succeeding operations. However, such simple classification method with a user-defined threshold may generate the problem of misclassification.

In order to correct the misclassified pixels, another classification method is proposed in [38], separating images into detail regions and smooth regions. In this method, the original image is divided into several blocks and the classification of each block depends

on the local gradient image by applying Prewitt operators. If the amplitude of the local gradient image is small, the block will be classified into smooth regions; otherwise it belongs to detail regions. In such case, the gradient threshold value is chosen as the first “dip” point of the distribution curve of the regional gradient mean, as shown in Figure 2.5(a). The block of which the gradient mean is less than the threshold will be classified into smooth regions. However, due to the small number of regions in an image, it is hard to detect the position of the “dip” point precisely without any misclassification, such as the situation displayed in Figure 2.5 (b).

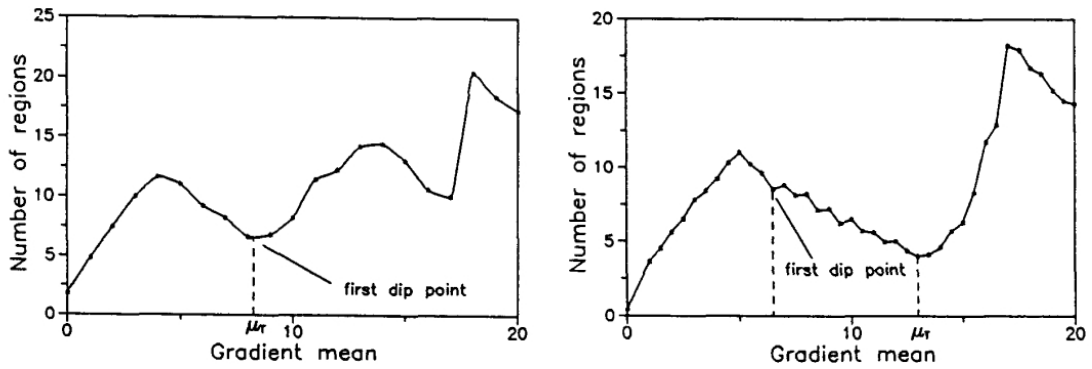


Figure 2.5. (a) The distribution of regional gradient means. The first “dip” point in the curve denotes the initial gradient threshold. (b) An example of misclassification [38].

In [38], two methods have been proposed to solve the problem of misclassification. The first one is smoothing the distribution curve. The second method tries to redefine the gradient threshold  $T_g$  by using the equation shown below

$$T_g = \mu_g + k_g \sigma_g ,$$

where  $\mu_g$ ,  $\sigma_g$  is the mean and standard variation of gradient amplitudes of all the pixels in smooth regions after classification,  $k_g = 3.5$ . A parameter is then introduced to classify all the blocks, its definition is

$$p_k = N_k / N_{\max}$$

where  $N_K$  is the number of pixels of which the gradient mean is larger than  $T_g$  in the  $k^{\text{th}}$  block,  $N_{\max}$  is the maximum value among all the  $N_K$ . Therefore, if its  $p_k < p_T$ , the block will be classified as smooth region, otherwise it belongs to detail regions.  $p_T$  is a user-defined factor.

In this way, the blocks will be classified to achieve a balance between the background noise removal and signal preservation. However, it is difficult to decide the value of  $p_T$  in order to minimize the probability of misclassification. For example, a too large value of  $p_T$  may increase its likelihood of misclassifying detail regions into smooth regions. It needs more manual observation and analysis for input images.

In the work presented in [36], a specific binary mask is used in each LP stage to protect the signal pixels and expose noise. The signal quality of the final image is related to the quality of the controlling masks, which are generated by the process of pixel classification. Thus, the essence of this approach is to design a good classification method to obtain high quality signal masks for different levels of protection/exposure. Figure 2.6 shows a schematic diagram of pixel classification followed by a region correction process [36].

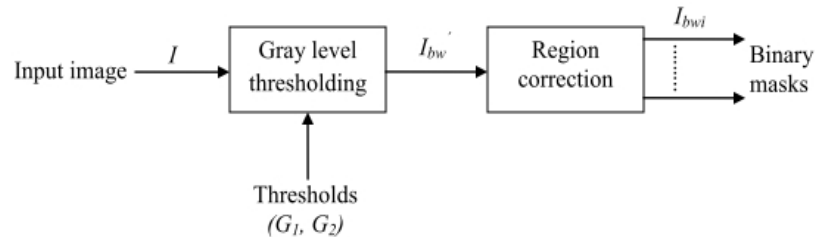


Figure 2.6. Pixel classification with region correction.

This classification method is based on the homogeneity of pixel locations. The first step is to group the pixels by gray level thresholding, i.e.,  $G_1$  and  $G_2$ . The pixels of which the gray level is between  $G_1$  and  $G_2$  will be classified as homogeneous pixels and others non-homogeneous ones. However, no matter how carefully one can choose the threshold values, there always exist a large number of misclassified pixels. Therefore, a region correction based on the pattern recognition is designed to locate those misclassified pixels. Once a misclassified pixel is confirmed, it would be assigned to its original class. [36] uses pattern recognition method to distinguish the patterns formed by non-homogeneous pixels from those of misclassified ones. It is known that a non-homogeneous region is unlikely to be one-pixel-wide. Therefore, if a classified region of non-homogeneous pixels is very thin, it is very likely to be formed by misclassified pixels and should be corrected into homogeneous regions. By applying such classification method, the concentration of pixel signals in non-homogeneous regions and that of noise in homogeneous regions will be increased greatly. Finally, after region correction, a series of binary masks containing different groups of pixels are generated and will be used in the multi-stage LP filtering process.

However, the classification process reported in [36] requires the users to manually select and adjust parameters, which makes the quality control less evident. To overcome this limit, an autonomous pixel classification method is required.

Many other approaches of pixel classification are also reported in [39]. However, any method of pixel classification stands a chance of misclassifying a certain portion of pixels.

Therefore, a precise and automatic pixel classification method is needed to minimize such chance for an effective noise removal and good signal preservation.

## ***2.4. Summary***

This chapter describes the main approaches of contrast enhancement. Some recent progresses on improving the traditional contrast enhancement methods are reviewed, which includes improved versions of the standard HE, post-CE denoising techniques and pixel classifications methods for generating signal-preserving masks. To develop a simple algorithm for a good contrast and low noise, after lots of research on the relevant work, the multi-stage low-pass filtering operation is, thus, introduced as the basis of the work presented in this thesis for its simplicity and effectiveness. The technical challenge of implementing this method is to develop an effective and precise classification method for a high-quality low-noise image. In next chapter, the algorithms of the pixel classification and its two applications in image processing are proposed and explained in detail, trying to achieve adaptive and autonomous generation of the signal-preserving masks.

# Chapter 3. Description of Proposed Algorithm

## 3.1. Overview

As described previously, contrast enhancement is essential in image processing and varieties of HE-based enhancement method have been reported. However, it is often the case that, while the signal contrast is enhanced, the image noise is also amplified. A lot of research efforts have been made to develop better adaptive HE algorithms. Nevertheless, it is hard to find a good solution to the conflict between contrast enhancement and noise generation. Using low-pass filters to remove HE-generated noise is an effective approach, as the two issues of the conflict are addressed separately. The critical point in this approach is, however, the conflict of noise removal and signal preservation. The multi-stage LP filtering involved in the contrast enhancement scheme [36] can be effective to remove the noise while preserving signal variation if the pixels can be well classified according to the homogeneity of their locations. The work presented in this chapter focused on developing simple and effective methods for the pixel classification.

It is known that the gray level homogeneity can be indicated by gradients [38]. One can use a simple gradient thresholding to classify, approximately, the pixels into two classes, i.e., those in homogeneous regions and those in non-homogeneous regions. As mentioned previously, if the gradient signals are degraded in a complex manner, such a simple classification may not be satisfactory. In order to achieve better results, the gradient-based classification should be made discriminative, i.e., pixels having the same

gradient value may be classified differently according to their signals and/or their positions in the image. To this end, the pixels need to be grouped, and the classification by means of the gradient analysis is then performed in each group. Therefore, a procedure to generate the control masks from the input image should involve HP filtering to generate the pixel gradients and pixel grouping for the pixel classification, as shown in Figure 3.1.

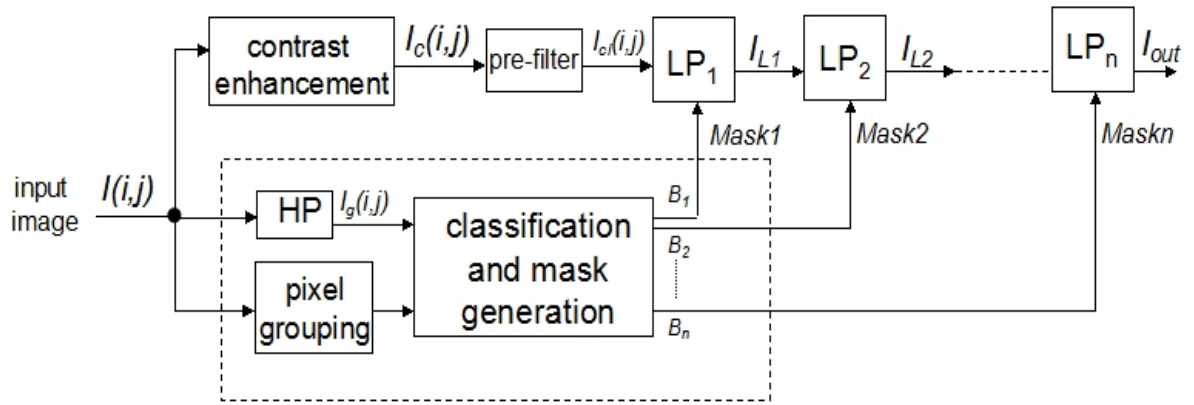


Figure 3.1. Schematic diagram of the proposed algorithm.

This chapter is organized as follows. In the following section, a simple gradient distribution analysis is described and the basic method to generate the thresholds for the classification is presented. In Section 3.3, an algorithm for the classification and mask generation aiming at HDR images is proposed. Another classification algorithm, also involving the basic method, is proposed in section 3.4. It targets a wider range of low contrast images.

### ***3.2. Analysis of the gradient distribution and the threshold generation for pixel classifications***

In order to perform an efficient low-pass filtering with gradient signal preservation, the pixels of an image need to be classified into groups, according to the homogeneity of their gray level variations of the regions where they are located. The pixels can be classified, for example, into three groups. The first one consists of homogeneous pixels, i.e., those located in homogeneous regions, the second one of non-homogeneous pixels, and the rest of the pixels form the third group. For clarity of the description of the classification method, it is assumed that the third group is divided into two sub-groups, one consisting of the pixels in near-homogeneous regions and the other found in near-non-homogeneous regions.

Gray level variations can be evaluated by the gradients obtained in a convolution with high-pass kernels, such as Sobel, detecting the gray level variation in the horizontal, vertical and diagonal directions. The method of the classification presented in this study is based on an analysis of the gradient distribution, i.e., the gradient histogram of the image.

In order to illustrate a typical gradient distribution, a SOBEL convolution is applied to a test image shown in Figure 3.2 (a) and the gradient map obtained is presented in Figure 3.2(b). The normalized histogram of the gradient is shown in Figure 3.3(a), and its outline represents the gradient distribution of the image.

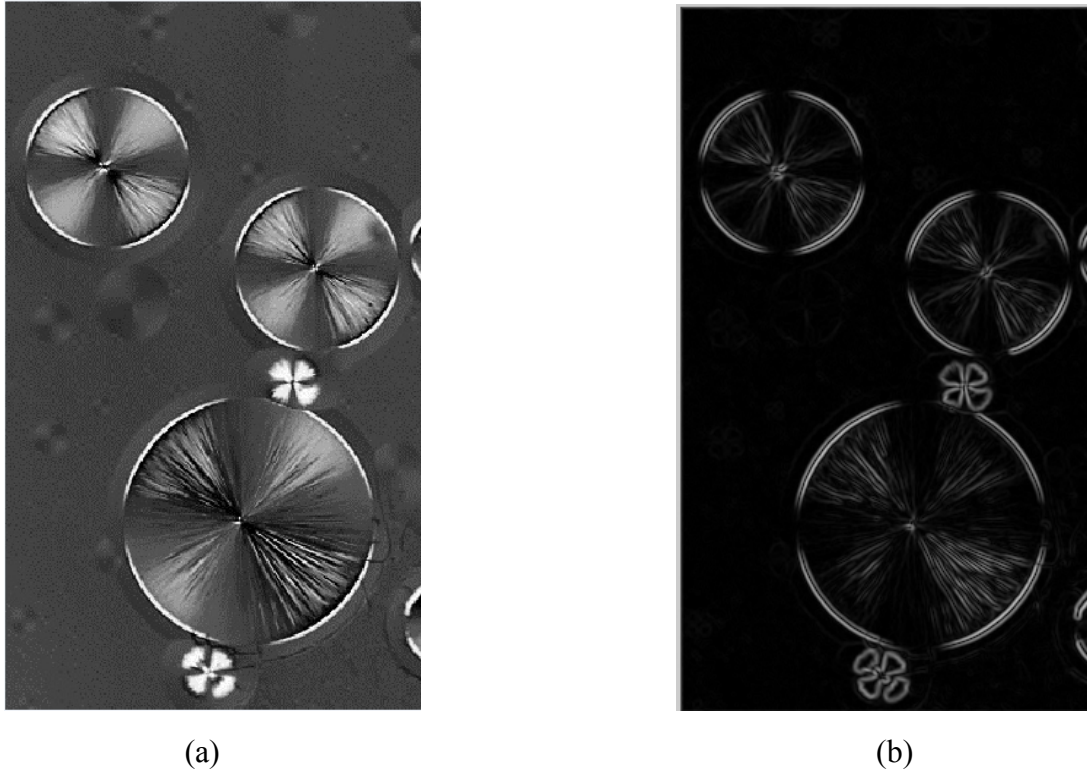


Figure 3.2. (a) Test image. (b) Gradient map of image (a).

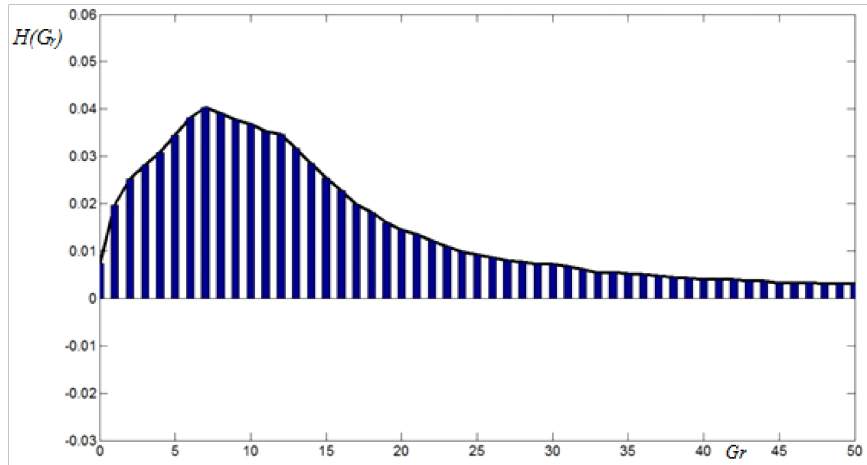
It is commonly known that the pixels having low gradient values are likely to be found in homogeneous regions, and those in non-homogeneous regions usually have higher gradient values. Hence, conceptually the pixels found in the left side are mostly homogeneous ones and those in the right side are non-homogeneous ones. However, to group the pixels more precisely, one needs to have a close observation on the distribution and its variation.

In order to classify the pixel population into the groups as stated above, three specific gradient values, denoting  $Th_L$ ,  $Th_M$ ,  $Th_H$ , should be identified. This gradient-based classification is presented in Table 3.1.

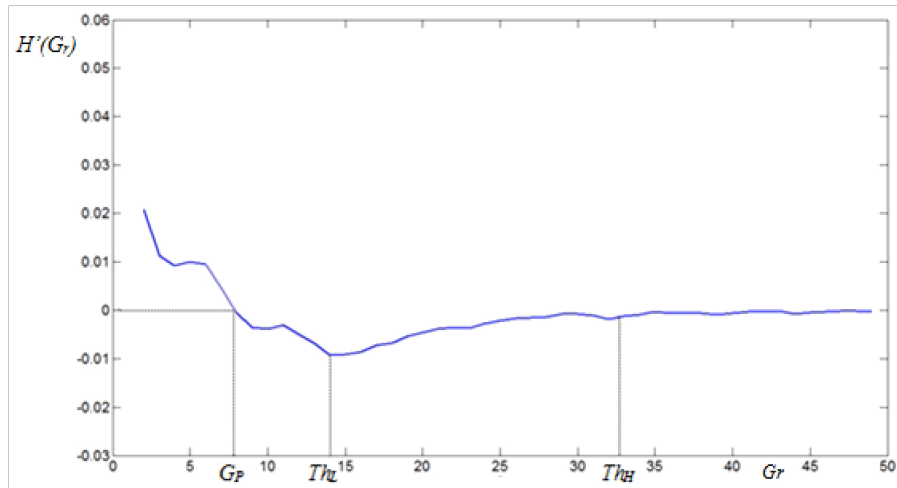
Table 3.1. Gradient based classification

<b>If</b>	<b><math>I(i,j)</math> is classified as</b>
$g_r(i,j) > Th_H$	homogeneous pixels
$g_r(i,j) < Th_L$	non-homogeneous pixels
$Th_L < g_r(i,j) < Th_M$	near-homogeneous pixels
$Th_M < g_r(i,j) < Th_H$	near-non-homogeneous pixels

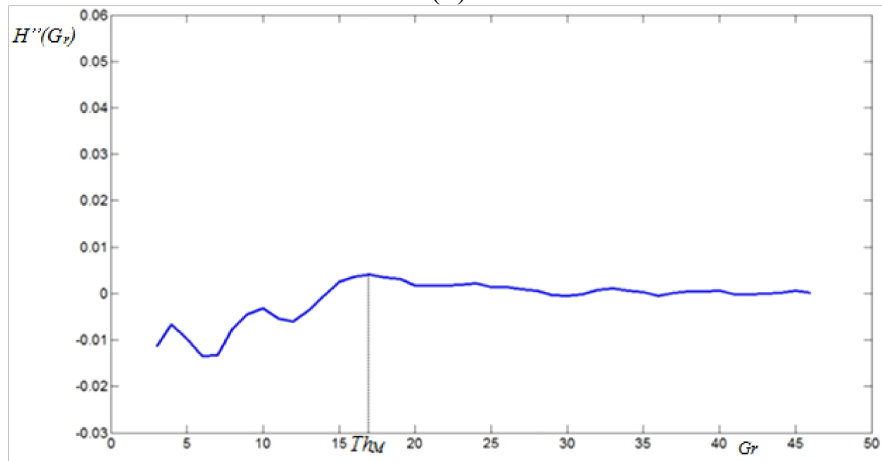
The gradient value of  $Th_H$  is to be used as a threshold to identify non-homogeneous pixels from the entire pixel population. Figure 3.3(a) shows that, the gradient distribution is relatively stable if the weighted gradient value is relatively large. The pixels having these gradient values are mostly non-homogeneous ones. To define the specific point  $Th_H$  in order to separate the section corresponding to those pixels from the rest of the curve, a first derivative of the distribution curve is obtained and presented in Figure 3.3(b). This derivative curve illustrates,  $\frac{dH(G_r)}{dG_r}$ , the change rate of the gradient distribution varying with  $G_r$ . If the weighted gradient value is much greater than 10, the derivative will approach zero from a negative value. Let us define  $Th_H$  as the gradient found at the point where  $|\frac{dH(G_r)}{dG_r}|$  is very close to zero, such as 0.001.



(a)



(b)



(c)

Figure 3.3. (a) Gradient distribution obtained from the gradient map shown in Figure 3.2(b). The y-axis is the normalized value of the distribution, and  $G_r$  of x-axis is the SOBEL-weighted gradient value, i.e., the height of the gradient bin. (b) First derivative of the outline curve presented in (a). (c) Second derivative of the outline curve presented in (a).

The low gradient homogeneous pixels are to be identified from the total pixel population by a threshold  $Th_L$ . In general,  $Th_L$  should be found between  $G_P$ , shown in Figure 3.3(b), and  $Th_H$ . In this segment of the distribution, the rate of the histogram changes sensitively with the gradient value, i.e.,  $\frac{dH(G_r)}{dG_r}$  varies from zero to its negative peak and approach to zero again. The specific point of  $Th_L$  should be found between the distribution segment of homogeneous pixels and that of near-homogeneous pixels. This value can reasonably correspond to the largest  $|\frac{dH(G_r)}{dG_r}|$  and  $\frac{d^2H(G_r)}{d^2G_r} = 0$ , shown in Figure 3.3(b).

The pixels having their gradient values between  $Th_L$  and  $Th_H$  are located neither in homogeneous regions nor non-homogeneous regions. However some of them carry features more like homogeneous pixels and others more non-homogeneous ones. The distribution segments corresponding to the two sub-groups, i.e., near-homogeneous pixels and near-non-homogeneous pixels are separated by  $Th_M$ . In the segment between  $Th_L$  and  $Th_H$ ,  $\frac{dH(G_r)}{dG_r}$ , the change rate of the gradient distribution, shown in Figure 3.3(b), is ranged from its negative peak to near-zero. The specific point of  $Th_M$  is found at the highest peak point in the second derivative of the distribution as shown in Figure 3.3(c).

Summarizing the above description, the generation of the three specific values,  $Th_L$ ,  $Th_M$ ,  $Th_H$ , is illustrated in the diagram shown in Figure 3.4. As these values serve in the classification presented in Table 3.1 as the thresholds, the procedure involving the histogram and derivation operations is referred to as the threshold generation. Applying

this procedure to the test image shown in Figure 3.2(a), one can obtain the three thresholds and then produce the three binary images shown in Figure 3.5.

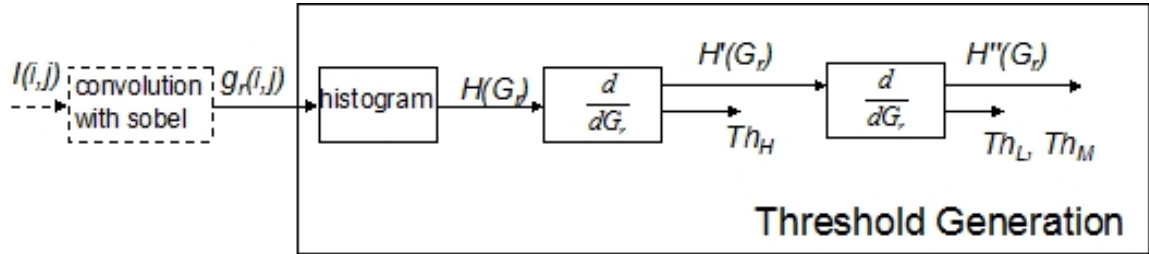


Figure 3.4. Procedure to define the three gradient values  $Th_L$ ,  $Th_M$ ,  $Th_H$  used in the gradient-based classification

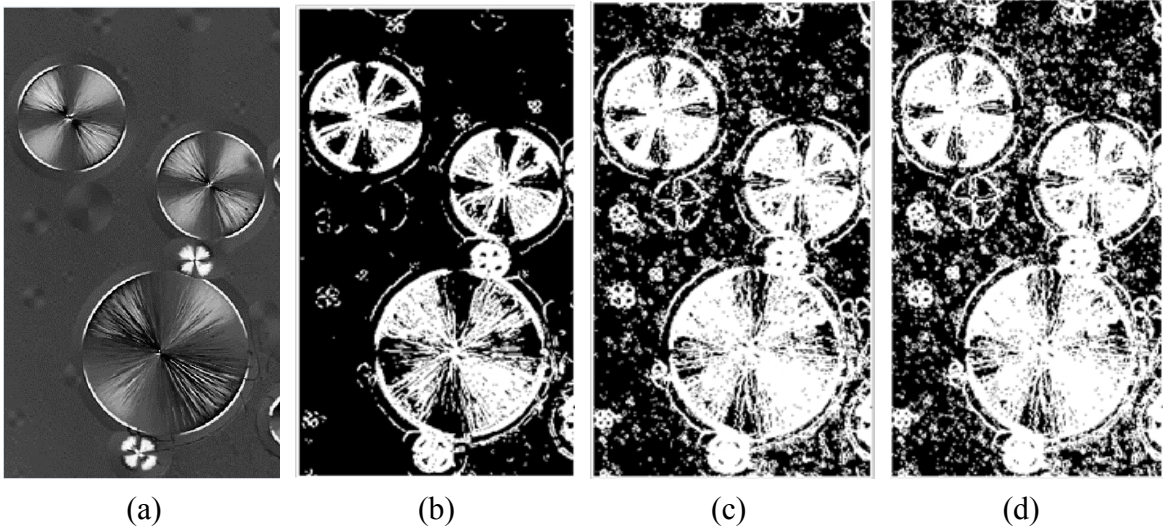


Figure 3.5. (a) Test image. (b) Mask generated by thresholding the gradient map of the image shown in (a) with the threshold  $Th_H = 38.8$ . (c) Mask generated by thresholding the gradient map of the image shown in (a) with the threshold  $Th_M = 17.1$ . (d) Mask generated by thresholding the gradient map of the image shown in (a) with the threshold  $Th_L = 14.9$ .

As described in §3.1, to implement the signal-preserving LP filtering, the masks for the protections of different pixel groups are needed. The first one protects only the non-homogeneous pixels, and the last one all the pixels except the homogeneous ones. Comparing Figure 3.5(a) and (b), one can find that, in the mask shown in (b), pixel positions in non-homogeneous regions have the logic-1 status, displayed as white dots,

while those in the rest of the image having the logic-0 status. This mask can be used to control the first LP stage shown in Figure 3.1. Contrary to Figure 3.5(b), the mask in Figure 3.5(d) is used to distinguish homogeneous pixels in (a) from the rest of the image, by marking the pixel positions of the former with the logic-0 status and the latter the logic-1 status. If the masks shown in Figure 3.5(b) and (d) are to identify the homogeneous and non-homogeneous pixel groups, respectively, the mask shown in Figure 3.5(c) is designed to distinguish the homogeneous and near-homogeneous pixels from the non-homogeneous and near-non-homogeneous ones. With this mask, the LP operation can be applied to all the homogeneous and near-homogeneous pixels.

In this section, a basic method for the threshold generation, based on the gradient distribution, has been presented. It has been shown that the gradient-based classification described above can be effectively used to generate binary masks for the signal-preserving LP filtering operations in the multiple stages as shown in Figure 3.1. The application of this simple method should be adaptive to the conditions of the input image. The gradient signal in an image of poor quality may be degraded in different ways depending on image features in different locations. In order to apply the basic method, the gradient distribution should be made “local” to facilitate the identification of the pixel groups. Hence, the pixels of the input image should first be grouped, according to a defined pixel features. And based on the gradient distribution of each pixel, the thresholds are found for the generation of the masks used in the LP filtering.

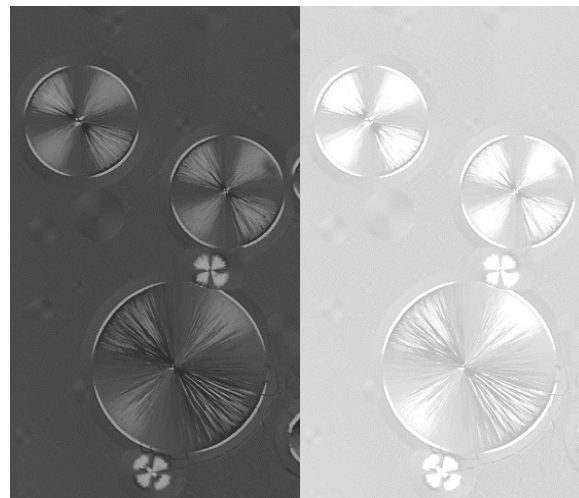
In the following sections, two algorithms, in which the basic method is applied to pixel groups, are presented. In each of them, the pixels are grouped based on different features and the control masks are generated accordingly.

### ***3.3. Classification algorithm with pixel grouping based on gray level ranges***

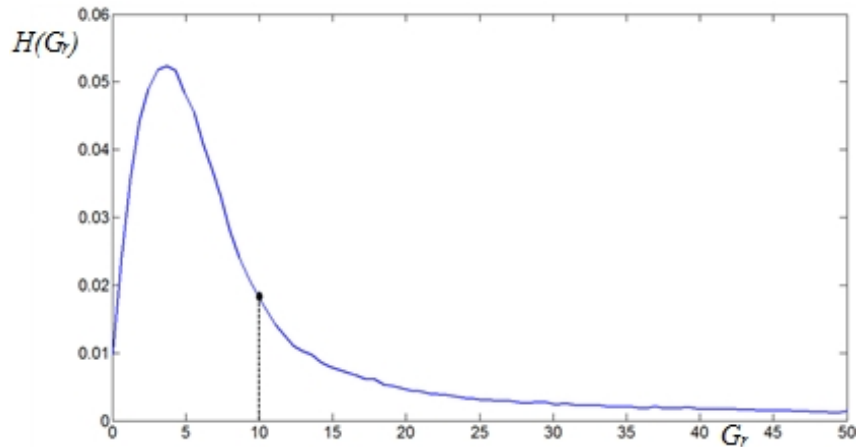
It is commonly known that in a high-dynamic-range (HDR) image, gradient signals may be degraded differently, likely depending on the intensity level. For example, a signal variation in a low intensity region or a gray level fluctuation in a median intensity region may yield gradient signals of the same level. In this case, in order to effectively apply the basic method of the threshold generation for pixel classification presented in §3.2, the pixels of the image need to be grouped according to its gray level, which correspond to the original intensity level.

Figure 3.6(a) illustrates an HDR test image. It is a combination of the two images of the same motives. One is under exposed and the other over exposed. The histogram of its SOBEL-gradients is shown in Figure 3.6(b). In this histogram, i.e., gradient distribution, the pixels in a gradient bin in a middle-range, e.g., those pixels having  $G_r = 10$ , can be in a bright homogeneous region or a darker non-homogeneous region. If the threshold values are generated from this distribution, the pixels in entire bin will be considered as homogeneous pixels or non-homogeneous ones. The binary masks produced

subsequently may not be able to serve the purpose of a threshold generation for gradient pixel classification. Hence one need to divide the gray level range of the image into some sub-ranges and to apply the method to a gradient distribution made from the pixels having their gray level values in the same sub-range. The threshold values based on such a distribution can thus be appropriate for the pixels. In this way, one can generate a set of masks in each sub-range. Combining it with other sets, one can produce a final set of masks for pixel classification of the entire image.



(a)



(b)

Figure 3.6. (a) An HDR test image. (b) Gradient distribution obtained from the gradient map of the image shown in (a).

For clarity purposes in the description, let us divide the gray level range of the input image into three sub-ranges, namely  $[ 0 , G_{L1} ]$ ,  $( G_{L1} , G_{L2} ]$  and  $( G_{L2} , 255 ]$ , and the pixels are grouped accordingly. The three gradient distributions can then be generated. One can obtain three thresholds from each of them, for example,  $Th_{L1}$ ,  $Th_{M1}$  and  $Th_{H1}$  from the gradient distribution of the pixels ranged from 0 to  $G_{L1}$ . The threshold  $Th_{L1}$  is then used to produce a binary mask  $B_{L1}$  in which the positions of all homogeneous pixels in the sub-image are indicated with the status of Logic-0, and the rest with Logic-1. Its counterparts in other two sub-images, i.e., the binary masks  $B_{L2}$  and  $B_{L3}$ , are produce in the same manner to identify the homogeneous pixels from the rest of the sub-images.

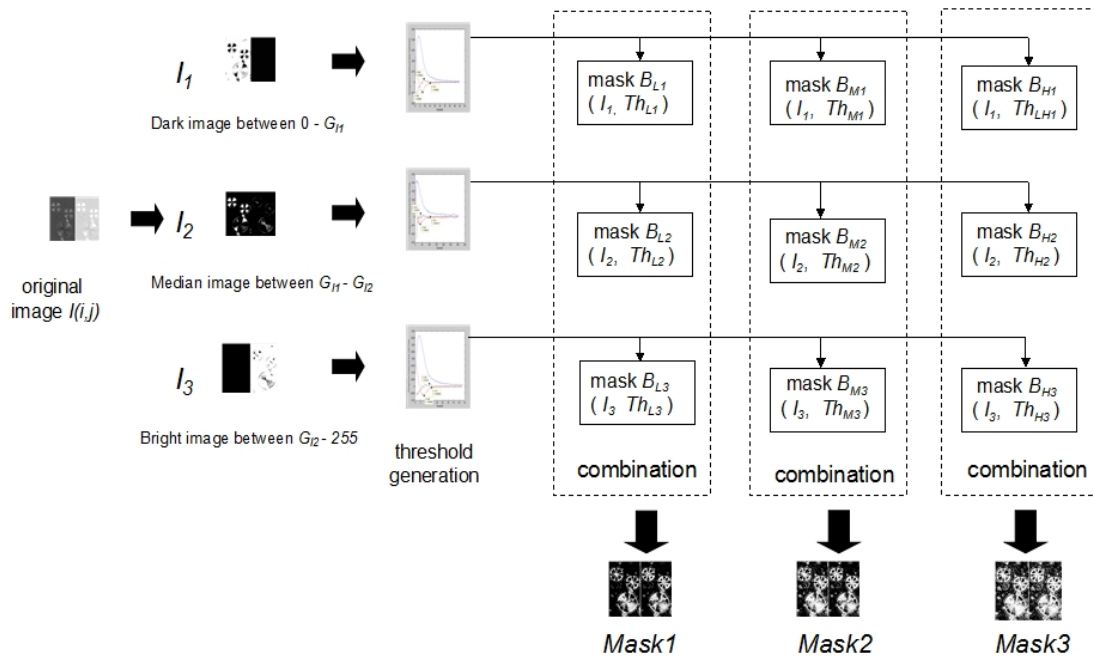


Figure 3.7. Process of mask generation

Figure 3.7 illustrates, in a conceptual manner, the process of the image data to demonstrate the algorithm of the pixel classification and mask generation. Combining the masks  $B_{L1}$ ,  $B_{L2}$  and  $B_{L3}$ , one can obtain a binary mask, namely  $Mask1$ , to distinguish the

positions of all the homogeneous pixels in the entire image from the rest of the pixel population. The two other masks are produced in a similar manner for the classification. All the three masks are to be used in the multi-stage low-pass filtering.

The block diagram of the algorithm for applying the gray-level-dependent local gradient distribution for pixel classification is shown in Figure 3.8. In this diagram,  $I_g(i,j)$  denotes the gradient map of the input image  $I(i,j)$ , and  $I_{g1}$ ,  $I_{g2}$  and  $I_{g3}$  are the local gradient maps of the sub-image, the detailed diagram of the classification block is found in Fig. 3.9 and that of the combination in Figure 3.10.

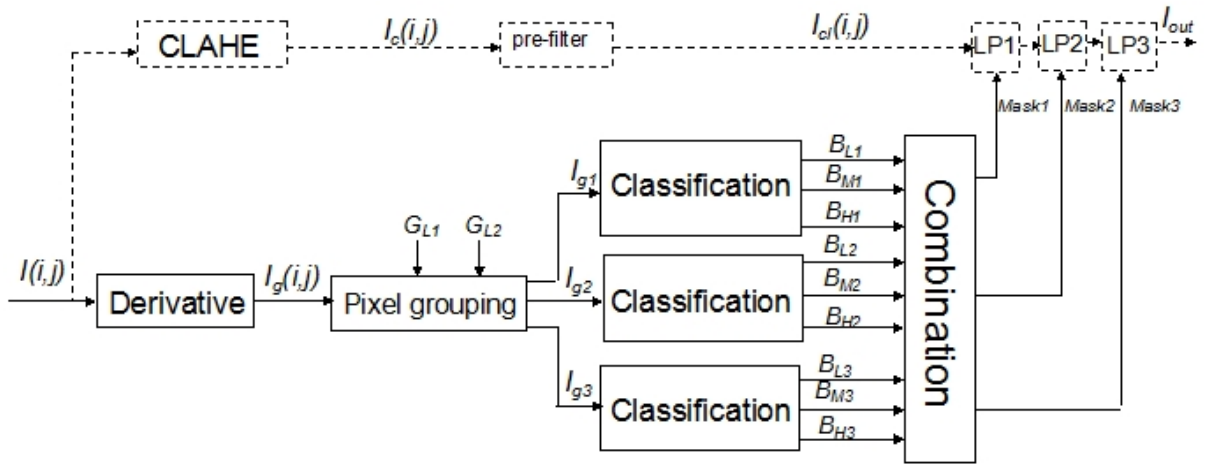


Figure 3.8. Block diagram of the algorithm for the pixel classification.

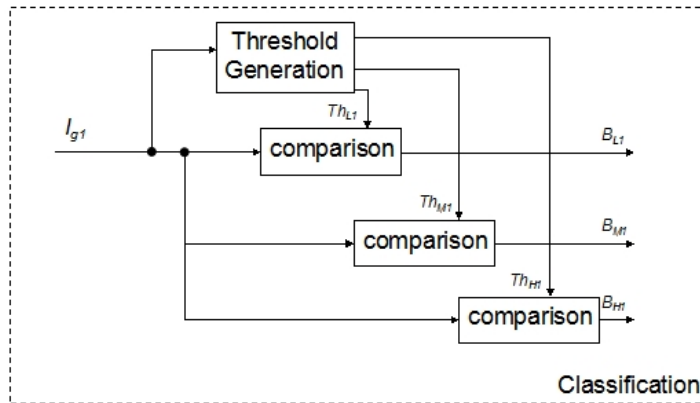


Figure 3.9. Block diagram of the classification shown in Figure 3.8.

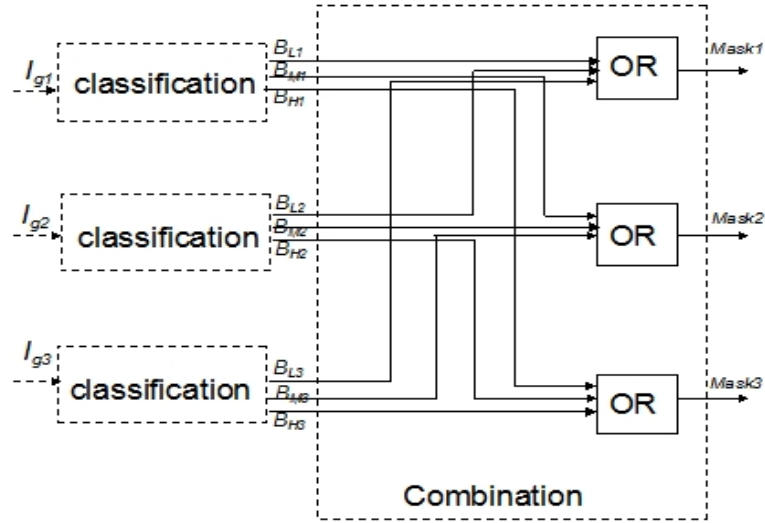


Figure 3.10. Block diagram of the combination shown in Figure 3.8.

Applying the algorithm presented in Figure 3.8 to the test image shown in Figure 3.6(a), with  $G_{L1} = 100$ ,  $G_{L2} = 200$ , one can obtain the three local SOBEL-gradient distributions of the sub-images shown in Figure 3.11. They are, in fact, the result of the decomposition of the global gradient distribution shown in Figure 3.6(b). In Figure 3.11(a), the global gradient distribution curve is placed with the three local ones. The three local gradient distributions are presented separately in Figure 3.11(b), (c) and (d) after the normalization with the total pixel number of the sub-image. One can see that the pixels in each bin in the global distribution are now sorted, according to their gray level, to form three segments, and placed in the corresponding bins of the three local distributions, respectively. The thresholds for each sub-images obtained based on the analysis of the three gradient distributions are displayed in Table 3.2. About 3% of the pixels in the global gradient distribution have  $G_r = 10$ , among these, only 0.1% are in the gray level range of  $[G_{L1}, G_{L2}]$ , forming the bin in Figure 3.11(c). They are classified as homogeneous pixels according to the threshold shown in Figure 3.11(c) and Table 3.2.

The other pixels make the bins of  $G_r = 10$  in Figure 3.11(b) and (d) will be considered as near-non-homogeneous pixels and near-homogeneous ones, respectively.

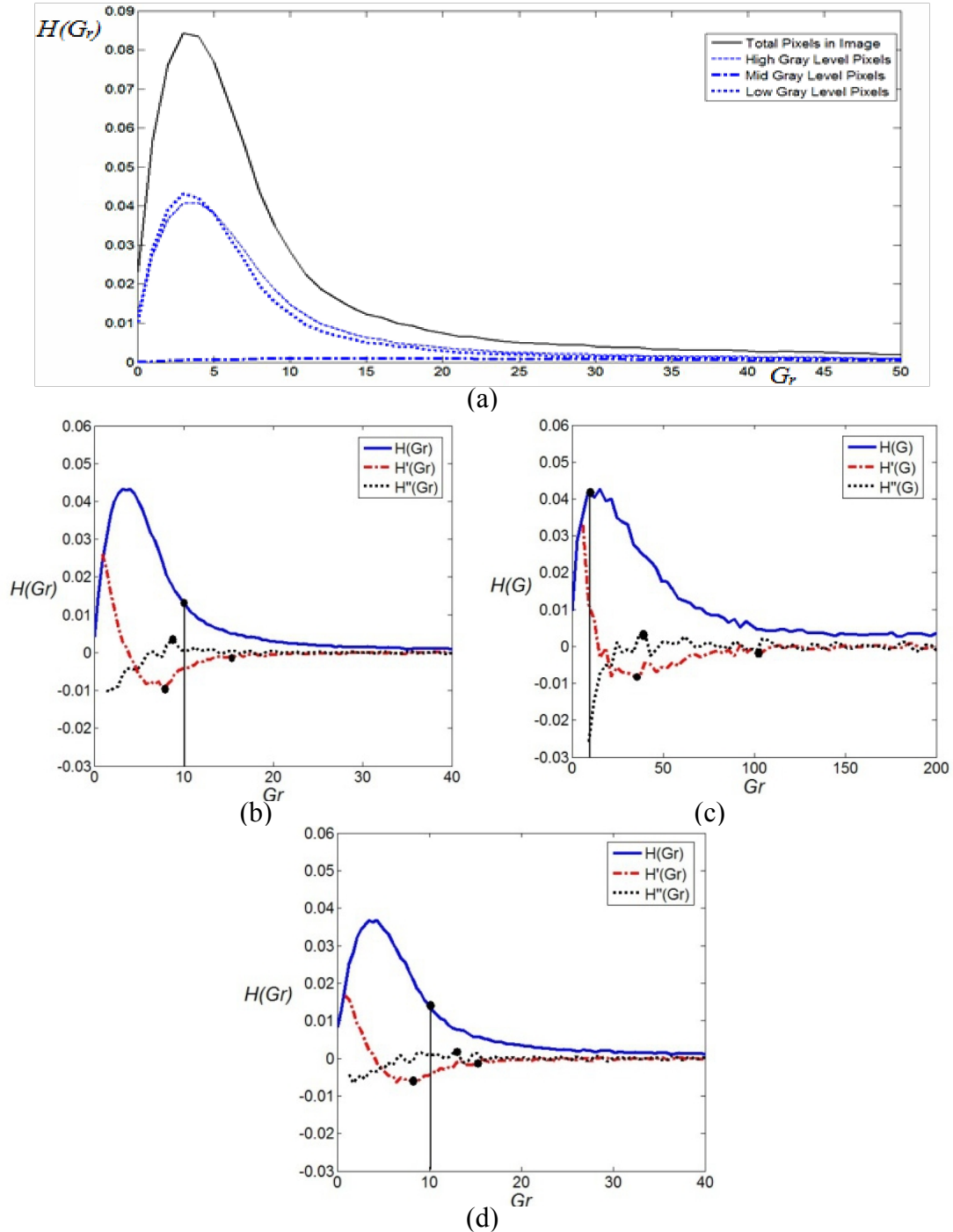


Figure 3.11. (a) Gradient distribution of the entire image displayed with the distributions of the three sub-images. (b) Local gradient distribution and its 1st order derivative for the pixels ranged from 0 to 100. (c) Local gradient distribution and its 1st order derivative for the pixels ranged from 101 to 200. (d) Local gradient distribution and its 1st order derivative for the pixels ranged from 201 to 255.

Table 3.2. Threshold values for pixel classification.

Threshold Value Gray Level Range	$Th_L$	$Th_M$	$Th_H$
$[ 0 , G_{11} ]$	$Th_{L1} = 7.7$	$Th_{M1} = 9.1$	$Th_{H1} = 15.31$
$( G_{11} , G_{12} ]$	$Th_{L2} = 37$	$Th_{M2} = 40.1$	$Th_{H2} = 107.9$
$( G_{12} , 255 ]$	$Th_{L3} = 8.2$	$Th_{M3} = 12.1$	$Th_{H3} = 15.2$

By a simple pixel grouping according to their initial gray levels, one can obtain a number of “local” gradient distributions. Each distribution corresponds to the local gray level condition and leads to a better threshold generation which should result in a significant improvement in the subsequent pixel classification.

As mentioned previously, the test image has two identical image motives placed side by side but the gradient signals are degraded non-linearly due to over-exposure and under-exposure condition. If the classification is satisfactory, the identified homogeneous regions in one side should be similar to those in the other side. The three masks obtained by applying the algorithm, shown in Figure 3.12, demonstrate that the proposed algorithm can produce such a classification result.

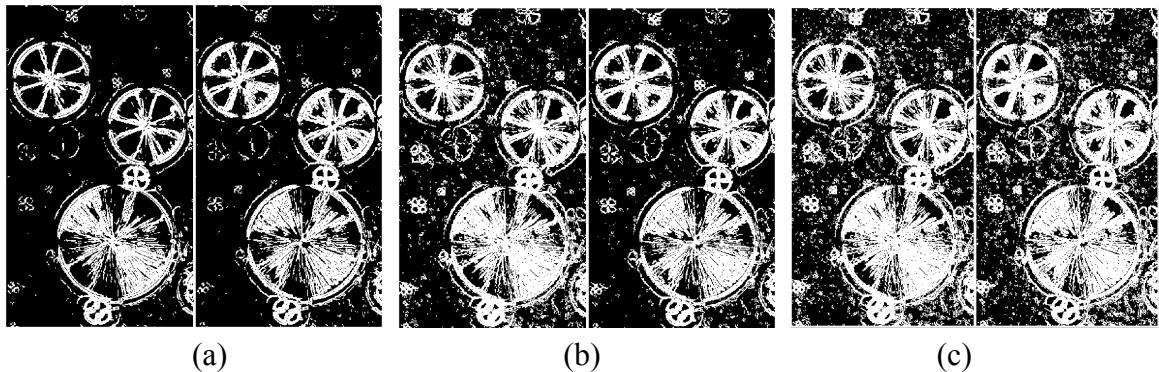


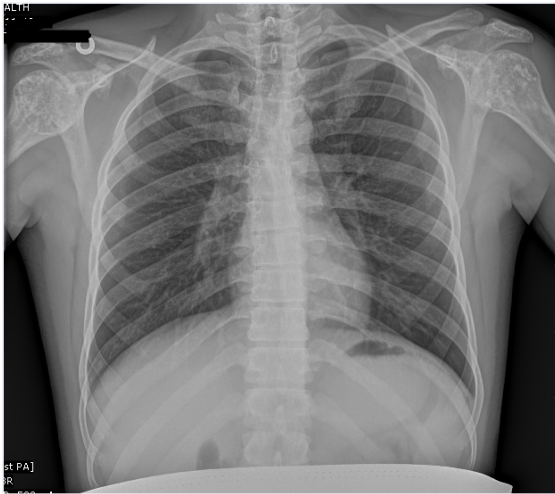
Figure 3.12. Masks obtained by threshold generation. (a) Mask corresponding to gradient level  $Th_L$ . (b) Mask corresponding to gradient level  $Th_M$ . (c) Mask corresponding to gradient level  $Th_H$ .

In this section, an algorithm for pixel classification in HDR images has been presented. In this algorithm, the basic method of the threshold generation based on the gradient distribution is applied. Aiming at gray-level-dependent gradient degradation, a pixel grouping by intensity range is incorporated to make the gradient analysis adapt to local gray level signals. Hence, one can expect a good classification result from the algorithm.

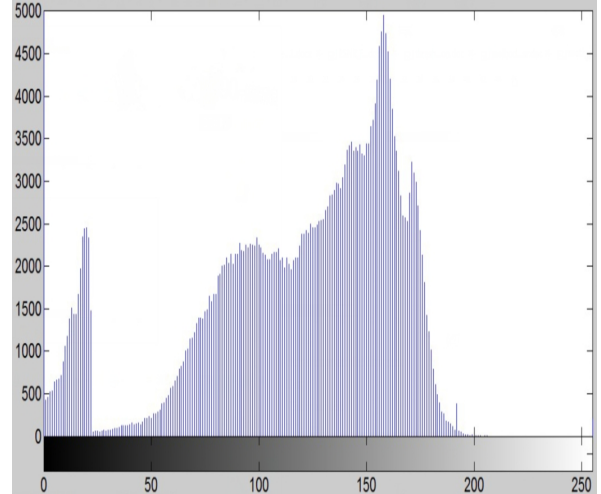
The basic method in §3.2 can be applied in a different way to target images having different features. In the next section, another algorithm, also involving this method, is presented.

### ***3.4. Classification algorithm with pixel grouping by histogram-thresholding***

In the algorithm proposed in §3.3, the pixels are grouped according to their original gray levels, if the gradient degradation is gray-level-dependent, and the algorithm is thus effective in case of HDR images. In many other cases, the image quality may be reduced by various causes, and the gradient signal degradation can be more complex than that in the cases discussed. In order to classify the pixels in terms of the gray level homogeneity, one wishes to group the pixels in such a way that the difference in gradients between the homogeneous pixels (or non-homogeneous pixels) and the rest of the population in the same group can be easily detected by applying the method presented in §3.2.



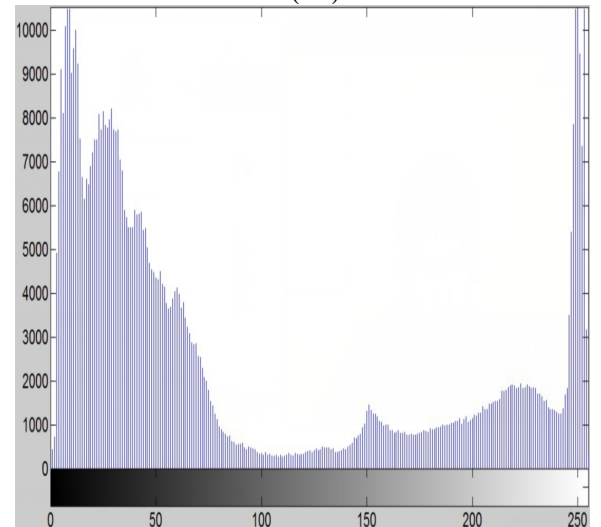
(a1)



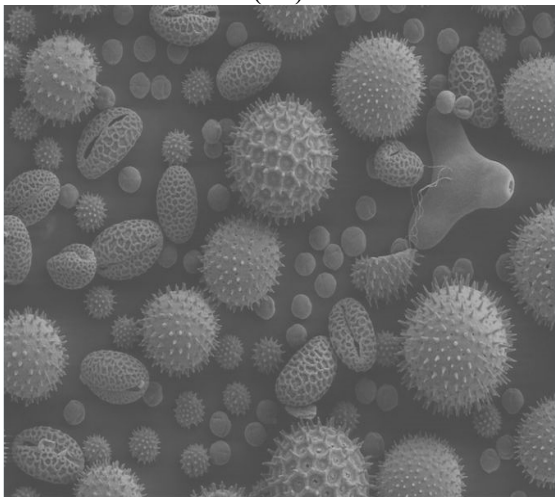
(a2)



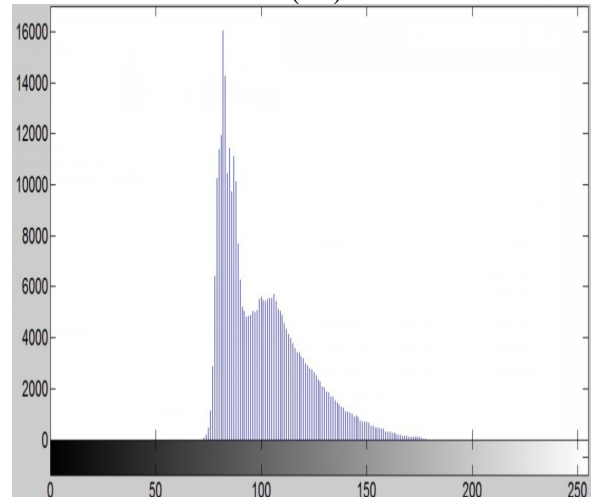
(b1)



(b2)



(c1)



(c2)

Figure 3.13. Low-contrast images and their histograms. (a1) (a2) X-ray. (b1) (b2) Window and Desk. (c1) (c2) Pollen Grain.

The histogram of an image illustrates its gray level distribution. Figure 3.13 shows three low-contrast images and their histograms. The gray level ranges of these images are very different, so are their textures, which results in different patterns in their histograms. However, one can easily see that in each of the histograms, the higher bins have a higher concentration of the homogeneous pixels. In other words, homogeneous pixels are more likely found in higher bins, and non-homogeneous ones in lower bins. If a histogram threshold  $T_G$  is applied to a typical gray level histogram, such as the one shown in Figure 3.14, the gray level bins will be divided into two groups. This is often referred to as histogram thresholding [24]. The dashed areas are composed of high bins, and include much more homogeneous pixels than the other bins of the histogram. It is to say that the pixels of the image are grouped according to the height of the bins, related to their likelihood to be homogeneous pixels. However while the majority of pixels in the high-bin group belongs to the class of homogeneous pixels, there is a minority of non-homogeneous pixels. In the low-bin pixel group, the situation is just in the opposite direction. If the gradients of the pixels of the minority in one group can be differentiated from those of the majority, those pixels will be easily identified. One can then apply the method of the gradient distribution analysis in each group to distinguish the minority pixels for a better pixel classification according to their gray level homogeneity.

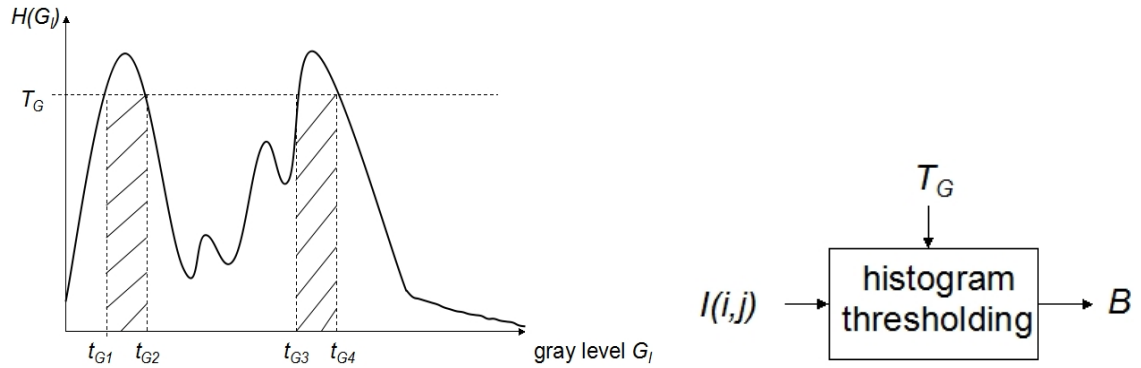


Figure 3.14. Histogram thresholding of an image to group the pixels. The binary mask  $B$  indicates the positions of the pixels in the undashed bins with Logic-1 status and the others Logic-0.

It should be mentioned that, in order to implement the preservation of signal variations in the low-pass filtering process shown in Figure 3.1, one needs to produce a binary mask for each LP stage. The mask controlling the first stage after the pre-filtering is to protect the non-homogeneous regions and expose the rest of the image. In other words, it is to distinguish the non-homogeneous pixels from the rest of the population. The non-homogeneous pixels are concentrated in the lower bins. Lowering  $T_G$  will group the lower bins together and exclude more homogeneous pixels from the group. Hence, to produce such a mask, a low-level  $T_G$  is applied to the histogram to increase the concentration of the non-homogeneous pixels of the un-dashed bins in the group in order to secure a good majority of likely-non-homogeneous pixels. In this case, the classification in this group is then to identify the minority homogeneous pixels by the gradient distribution analysis. Meanwhile, the majority of the pixels of the dashed-bin group are considered to be homogeneous pixels. To find the minority non-homogeneous pixels in that group, the same analysis is applied. Combining the results of the two classifications in the two groups, the mask identifying non-homogeneous pixels in the

image can be obtained. The other masks used in the LP process can be produced in a similar way. For example, the mask controlling the last LP is to expose only homogeneous pixels and protect the rest of the image. In this case the threshold  $T_G$  should be as high as possible to secure the majority pixels of the dashed bins likely being homogeneous ones.

Summarizing the analysis presented in the preceding paragraph, one can see that a simple histogram thresholding can be used to divide the pixels in an image into two groups, i.e., high-bins and low-bins. Each has a majority class and minority one, as presented in Table 3.3. By this grouping, each pixel position carries a logic status indicating which class it belongs to.

Table 3.3.

	Dashed-bins	Undashed-bins
Logic status before classification	"0"	"1"
Majority class	likely homogeneous pixels	likely non-homogeneous pixels
Minority class	non-homogeneous pixels and the rest	homogeneous pixels and the rest

Table 3.3 demonstrates the pixel grouping with a view to classifying the pixels to generate a binary mask for the protection of a particular group of pixels. As described previously, the histogram threshold  $T_G$  can be adjusted to pre-determine the concentration

of the homogeneous pixels or other kinds of pixels in a group. Aiming at the objective of a protective mask to be designed, the value of  $T_G$  should be chosen appropriately. By applying multiple  $T_G$  values, one can generate multiple binary masks for the multiple LP stages.

The above-described algorithm of the pixel grouping and classification for the mask generation can be presented in the block diagram shown in Figure 3.15. In this algorithm, each of the thresholds  $T_{G1}$ ,  $T_{G2}$  and  $T_{G3}$  is applied to the histogram of the input image, which results in three binary images, namely  $B_1$ ,  $B_2$  and  $B_3$ . The binary images are then applied individually to the gradient map  $I_g(i,j)$ . In each application  $I_g$  is divided into two groups, such as  $I_{g1-0}$  and  $I_{g1-1}$  in case of applying  $B_1$ . The pixel classification to be done in each of the groups is illustrated in Figure 3.16.

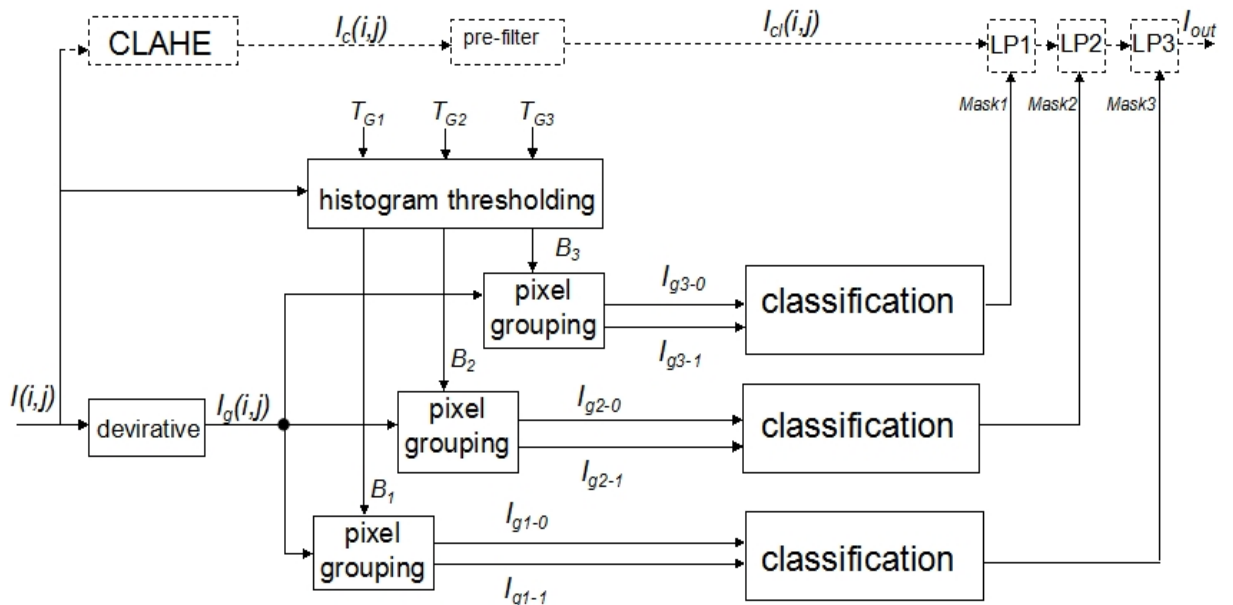


Figure 3.15. Block diagram of Algorithm 2.

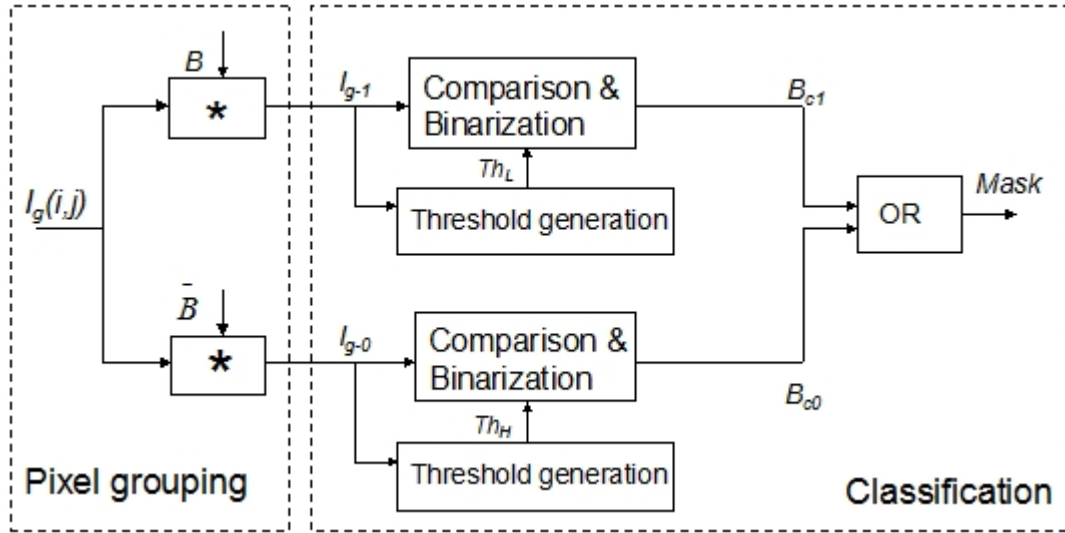


Figure 3.16. Detailed block diagram of the pixel grouping and the classification in the diagram shown in Figure 3.15.

As shown in Figure 3.16, the pixel gradient data is divided into two groups, i.e.,  $I_{g-0}$  and  $I_{g-1}$ , and each is to be binarized in the classification. The classification in each group is to identify the minority pixels. The identification is done by the analysis of the gradient histogram, such as the one shown in Figure 3.17, of the pixels in the group. For the group of  $I_{g-1}$ , the majority pixels are in the non-homogeneous regions. The classification is to identify the minority homogeneous pixels and to switch their logic status from Logic-1 to Logic-0. The gradient threshold is chosen, with precaution, to be  $Th_L$ , the lowest among the three threshold values shown in Figure 3.17, to exclude likely-non-homogeneous pixels, while minimizing the misclassification and a mask  $B_{c1}$  is then generated. In the group  $I_{g-0}$ , the pixels in the non-homogeneous regions need to be identified from the majority ones that are located in the homogeneous regions. The threshold, in this case, is chosen to be the highest, i.e.,  $Th_H$ , among the three values. Finally the two masks  $B_{c0}$  and  $B_{c1}$  are combined to form the mask used in a low-pass stage.

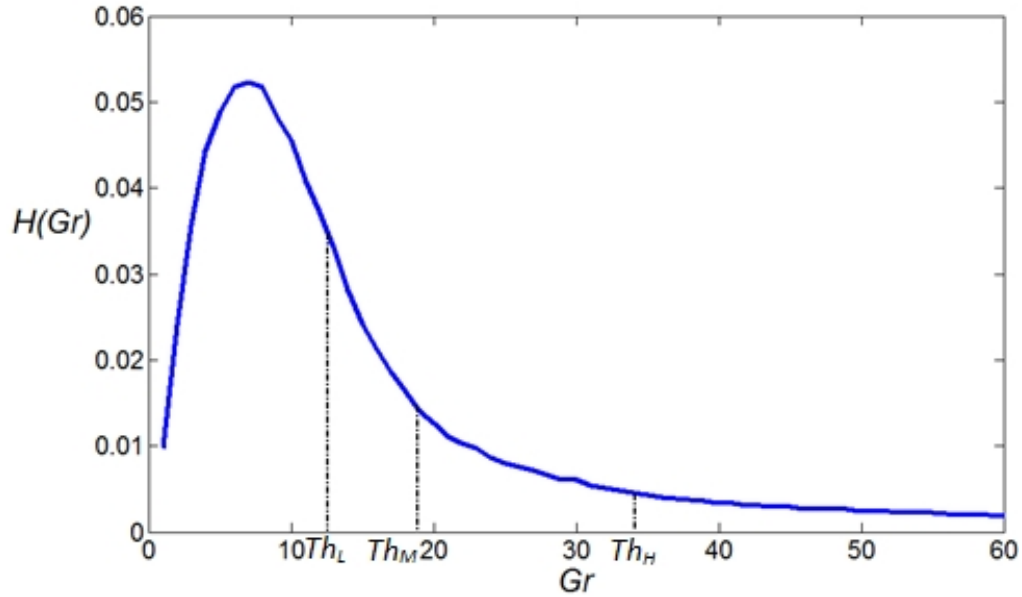


Figure 3.17. Example of the gradient distribution of a pixel group.

In order to generate the three masks, namely *mask 1*, *mask 2* and *mask 3*, shown in Figure 3.15, three values of  $T_G$ , i.e., 10%, 30% and 80% of the maximum of the bin-height in the histogram have been chosen, as shown in Figure 3.18(a). Consequently, three pairs of gradient maps have been obtained from the same  $I_g$  of the test image. The gradient histogram of one of the three pairs is shown in Figure 3.18(b) obtained by applying  $T_G$  of 30% of the highest bin. One can see in Figure 3.18(b) that the pixel grouping results in a decomposition of the global gradient distribution into two distinguished gradient characteristics. The two thresholds, i.e.,  $Th_L$  and  $Th_H$ , obtained from the two gradient characteristics, respectively, are used to generate the mask to be used in one of the stages. The pixels, of which the gradient values are in the range of  $(Th_L, Th_H)$ , are classified discriminatively according to the group to which they belong. Those in the high-bin group maintain their Logic-0 status as they are highly probably to be the

majority homogeneous pixels. Similarly, those in the low-bin group remain as non-homogeneous ones.

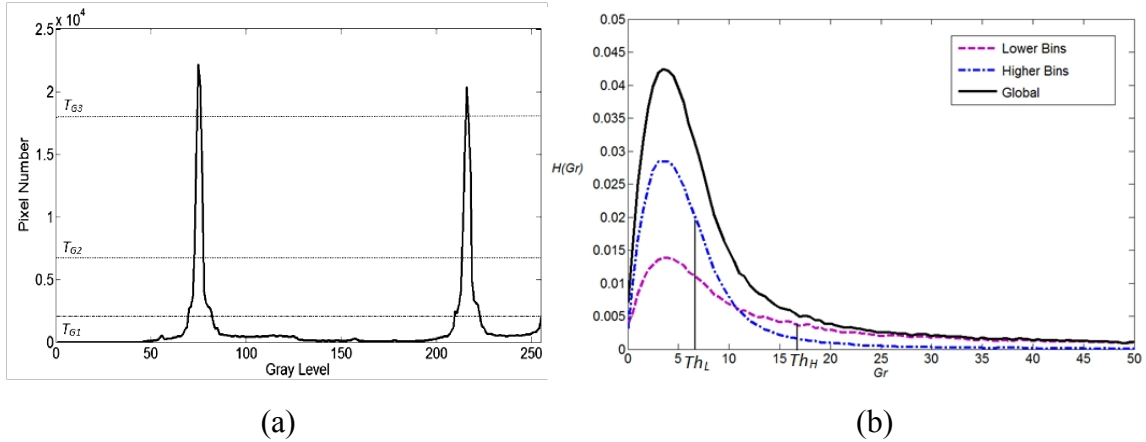


Figure 3.18. (a) Histogram of the test image shown in Figure 3.6(a). (b) Gradient distributions of  $I_g$ . The solid curve is given by the pixels of the entire  $I_g$ . When the pixels are grouped with  $T_{G2}$ , which is 30% of the maximum height, the low-bin group yields the dashed curve and high-bin group the dot-dashed one.

The gradient distributions with other values of  $T_G$  are, in principle, similar to those shown in Figure 3.18(b). The same procedure has been applied for the pixel classification and mask generation for the other LP stages. The masks illustrated in Figure 3.19 are the results of this application of the algorithm to the test image. They can provide the low-pass stages with different levels of protection/exposure.

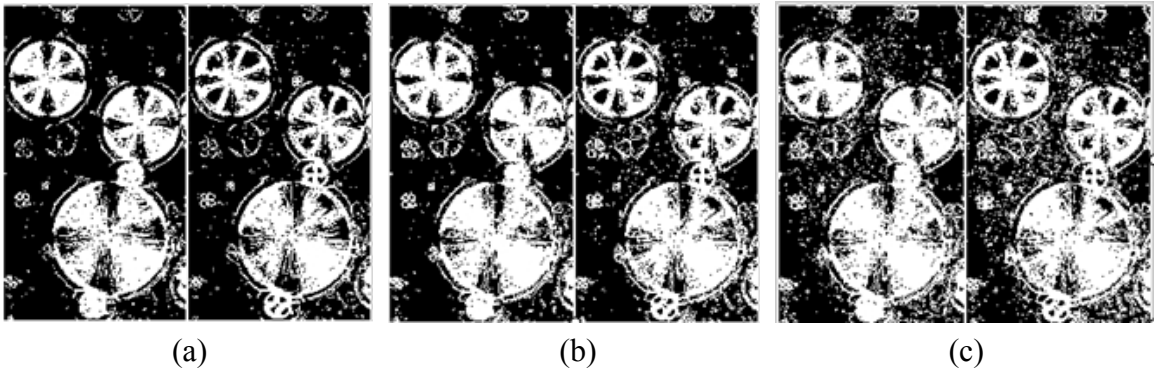


Figure 3.19. Binary masks obtained by applying the algorithm 2. They can be used in the procedure shown in Figure 3.15. (a) *Mask 1*. (b) *Mask 2*. (c) *Mask 3*.

The work presented in this section is to propose a simple algorithm for pixel classification targeting a wide range of low-contrast images of different motives/textures in which signal gradients may be degraded by various causes. In this algorithm, the method of the gradient distribution analysis presented in §3.2 is applied. To make the application effective to an image with complex gradient attenuations, the pixels are grouped according to their positions in the gray-level histogram bins, which implies their likelihood to be homogeneous (or non-homogeneous) pixels. By this grouping, the signal gradients of the pixels can be differentiated from those of the background fluctuations, and homogeneous pixels and non-homogeneous ones can be distinguished easily in each group by applying the simple gradient distribution analysis. One example of applying the algorithm has been presented and the results have shown the effectiveness of the proposed algorithm.

### ***3.5. Summary***

The objective of the work presented in this chapter is to develop simple and effective methods for the pixel classification according to the homogeneity of the regions where they are located. The two classification algorithms proposed in this chapter aim at low-contrast images where gradient signals are severely degraded. In each of the two, a high-pass filtering is involved. Base on a simple analysis of the subsequently generated gradient distribution, the special gradient values that can be used as thresholds in the

pixel classification are then determined. One of the algorithms has been developed to target HDR images. The pixels are first grouped according to their gray level ranges, as the gradient degradation is, in such a case, gray-level dependent. The analysis can then be done with the gradient distribution of each sub-image with a view to a pixel classification adapting to their original gray level signals. The other algorithm proposed is to tackle a wider range of low-contrast images. It has a simple computation procedure. In this algorithm, a gray-level histogram thresholding is performed to group the pixels according to their likelihood to homogeneous, or non-homogeneous groups, which establishes a majority of homogeneous/non-homogeneous pixels in each group. The classification done in the group is to identify those in the minority. The applications of the two algorithms to a test image have also been presented to illustrate how they can be used easily and promising results can be observed. Application to other low-contrast images and the analysis on the results are presented in the following chapter.

# Chapter 4. Simulation Results and Evaluations

## ***4.1. Introduction***

The MATLAB simulation is carried out to evaluate the effectiveness of the proposed algorithms described in Chapter 3. The assessment of the performance involves subjective observations of the processed images and objective measurements for noise removal and edge preservation. These results are compared with those obtained by some of the advanced methods relevant to the work.

This chapter consists of two sections. In the first section, the simulation conditions are described and the parameters presented. The objective performance metrics used in the assessment are also presented. The simulation results and comments are found in the second section.

## ***4.2. Simulation conditions***

The simulation of the procedure shown in Figure 3.1 has been performed with MATLAB. The algorithm of CLAHE is used in the block of contrast enhancement. In this block, the tile size is 8 x 8 pixels and clip limit is 0.03 in order to obtain a good contrast enhancement. All the low-pass filters are Gaussian. The first one, i.e., the pre-filter, is placed to perform a weak smoothing operation to the entire image. It has its window sized 3 x 3 pixels and  $\sigma = 0.5$ . The other LP filters have 5 x 5 windows and  $\sigma = 1.0$ ,

each providing a moderate smoothing operation. The four SOBEL kernels, detecting the gray level variation in the horizontal, vertical and diagonal directions, are used in the HP block to obtain the weighted gradients.

In the simulation, the two proposed algorithms are involved in the procedure. For Algorithm 1, the gray level thresholds for the pixel grouping are  $G_{L1} = 100$  and  $G_{L2} = 200$ . In case of Algorithm 2, the histogram thresholds are chosen to be 10%, 30% and 80% of the maximum of the bin-height in the gray level histogram.

The simulation results are compared with those obtained by using two high-quality contrast enhancement methods. One is the iterated TMR filtering [1]. It uses LP filtering to remove the noise generated in histogram equalization, a similar approach to that of the proposed algorithms to the improvement of the image quality. The other method is an adaptive histogram clipping CLAHE for contrast enhancement [29], in which signal variance is used in the histogram equalization to reduce the noise effectively.

The contrast enhancement procedure involving the two proposed algorithms have been applied to three low-contrast images of different dynamic ranges and different characters, as they are acquired from different sources, one of X-ray, another one microscopic, and the other of high dynamic range scene. The simulation results, including those obtained by the two above-referred methods, are also presented in the next section.

To assess the effectiveness of noise removal and signal preservation of the LP filtering with the masks generated by the proposed algorithms, Peak Signal to Noise Ratio (PSNR) and Pratt's Figure of Merit (PFOM) are measured for the objective

evaluation. The PSNR is given by the following expression.

$$PSNR = 20 \log_{10} \left( \frac{I_{\max}}{\sqrt{MSE}} \right),$$

where  $MSE = \frac{1}{mn} \sum_{i=0}^{m-1} \sum_{j=0}^{n-1} [I_r(i, j) - I_e(i, j)]^2$ ,  $I_{\max}$  is the maximum possible pixel value of

the processed image,  $I_r$  and  $I_e$  are the reference and processed image, respectively.

Pratt's Figure of Merit (PFOM) [40] is calculated based on a comparison of the reference edge map and that of the image to be evaluated. It is defined as,

$$PFOM = \frac{1}{I_N} \sum_{i=1}^{I_F} \frac{1}{1 + \alpha d_i^2},$$

where  $I_N$  is the maximum value from the reference edge map and that of the processed image,  $I_F$  is the number of edge points found in the latter,  $\alpha$  is a scaling constant usually set to 1/9 [40] and  $d_i$  is the distance between the position of a found edge point and corresponding one in the reference edge map.

### **4.3. Simulation results**

The input images used in the MATLAB simulation are of very poor contrast, and thus require a good contrast enhancement, which is a challenge in the processing quality. In each of the four procedures, i.e., the iterated TMR filtering [1], the adaptive clipping [29] and those with two proposed algorithms, CLAHE is used to obtain a good contrast enhancement. It makes, however, the noise more pronounced in the enhancement process.

The final results illustrate how much different the LP filtering operations, or the adaptive clipping, can solve this problem of noise generated in the CLAHE process.

Figure 4.1 illustrates the simulation results of the different procedures applied to the image of “X-ray”. One can easily see the noise in the image processed by CLAHE in Figure 4.1(b). The image shown in Figure 4.1(c) is the result of the iterated TMR filtering. There is much less noise compared with that in Figure 4.1(b) but some signal details are also erased by the filtering. The adaptive clipping is to reduce the noise generation in the CLAHE process. It results in a contrast enhanced image, shown in Figure 4.1(d), with less noise than that in (b). However, the noise is still visible as there is a limit for the noise reduction and contrast enhancement if one attempts to achieve both in the same enhancement process. The images shown in Figure 4.1(e) and (f) have a significantly better quality, compared to that in (c) or (d). Each shows more signal details and much less noise. The good selectivity of the multi-stage low-pass filtering operation, resulting from the proposed algorithm for the pixel classification, has been proven effective to yield a good quality.

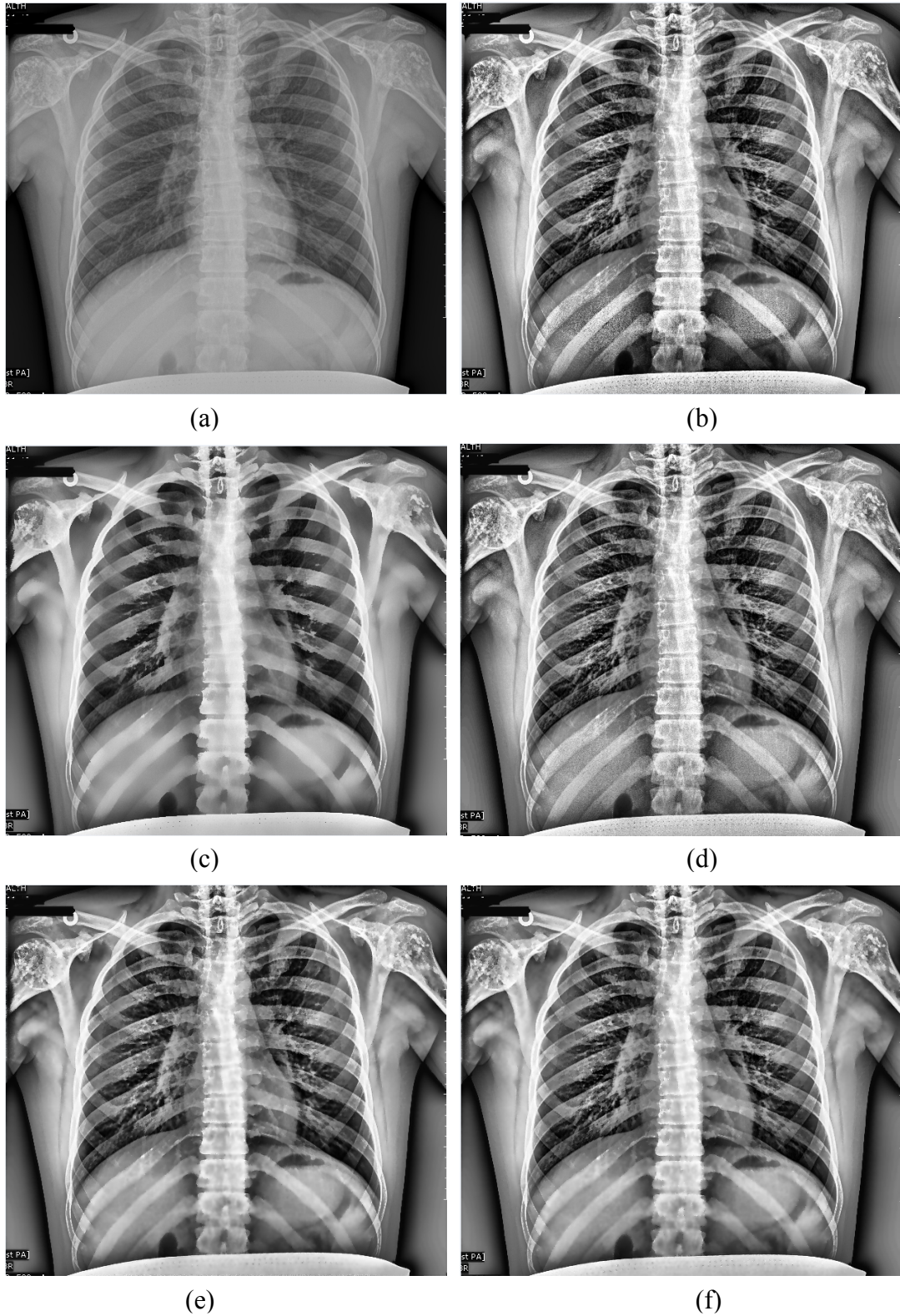
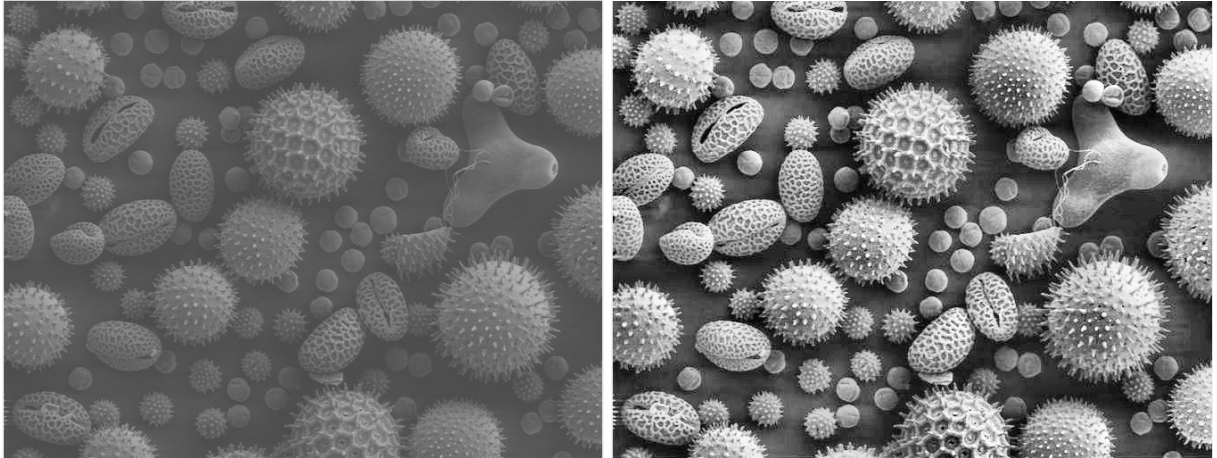


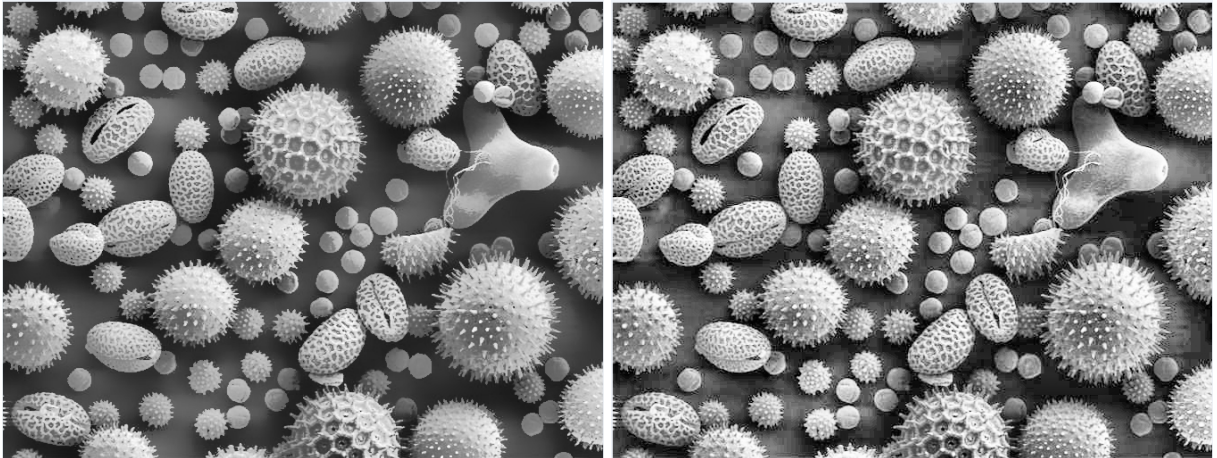
Figure 4.1. (a) Original image of X-ray. (b) By CLAHE. (c) By CLAHE combined with the iterated TMR filters. (d) By the adaptive clipping method. (e) By the procedure involving the proposed algorithm 1. (f) By the procedure involving the proposed algorithm 2.

The low contrast image shown in Figure 4.2(a) contains fine details, i.e., high spatial frequency components. After the CLAHE process, the noise is generated in the image, particularly around the boundaries of small objects. Similar to the results shown in Figure 4.1, one can see, by comparing Figure 4.2(e) & (f) with (c) & (d), the better noise removal and signal preservation given by the proposed algorithms.



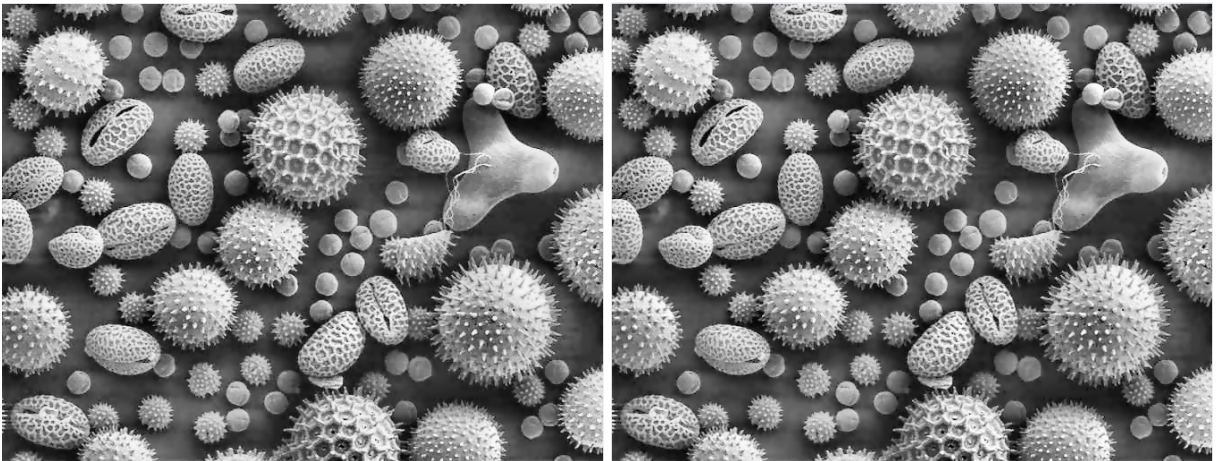
(a)

(b)



(c)

(d)



(e)

(f)

Figure 4.2. (a) Original image of Pollen Grain. (b) By CLAHE. (c) By CLAHE combined with the iterated TMR filters. (d) By the adaptive clipping method. (e) By the procedure involving the proposed algorithm 1. (f) By the procedure involving the proposed algorithm 2.

The image shown in Figure 4.3(a) is acquired from an HDR scene. It contains both under-exposed and over-exposed areas, and is thus chosen to test the effectiveness of the proposed algorithms in HDR cases, even though one of them is not designed specifically for HDR images. The CLAHE process makes a significant improvement in the image contrast, as shown in Figure 4.3(b), but the noise is also visible in the areas of high spatial frequencies, such as the clusters of the pens placed in the lower-left part of the image or around the edges of the bowl placed in the right side of the picture frame. The iterated TMR filtering gives a good smoothing effect, but it is visibly overdone with signal variations as shown in Figure 4.3(c). Compared with the image processed by the adaptive clipping, both proposed algorithms yield significantly better results, in terms of noise removal in the high frequency areas, as shown in Figure 4.3(e) and (f), while preserving signal variations in the image.



(a)



(b)



(c)



(d)



(e)



(f)

Figure 4.3. (a) Original image of Window and Desk. (b) By CLAHE. (c) By CLAHE combined with the iterated TMR filters. (d) By the adaptive clipping method. (e) By the procedure involving the proposed algorithm 1. (f) By the procedure involving the proposed algorithm 2.

From the observation of the images processed by the different procedures and the comparison of the results, it is obvious that the two proposed algorithms leads to visibly a better quality of the image contrast enhancement procedure, in terms of noise reduction and signal preservation. The objective measurements, i.e., PSNR and PFOM, are carried out with the images “Window and Desk” and “Pollen Grain”. The PSNR values are obtained by using CVIP tools [22]. The results are displayed in Tables 4.1 and 4.2. It is shown that the two proposed algorithms yield better PSNR and PFOM compared to those given by the adaptive clipping. The iterated TMR filtering produces a similar PSNR to those from the proposed algorithms, but its process gives a lower PFOM, reflecting its limitation in the edge preservation. These results confirm the conclusion obtained from the examination of the processed images.

Table 4.1. PSNR of the iterated TMR filtering, adaptive clipping and the two proposed algorithms.

Method Input image	PSNR				
	CLAHE	Iterated TMR filtering	Adaptive clipping	Proposed algorithm 1	Proposed algorithm 2
Window and Desk	18.060	18.347	18.438	18.472	18.377
Pollen Grain	11.697	12.075	12.024	12.078	12.077

Table 4.2. PFOM of the iterated TMR filtering, adaptive clipping and the two proposed algorithms.

Method Input image	PFOM			
	Iterated TMR filtering	Adaptive clipping	Proposed algorithm 1	Proposed algorithm 2
Window and Desk	0.895	0.899	0.934	0.926
Pollen Grain	0.873	0.960	0.971	0.970

Table 4.3 displays the elapsed time for MATLAB simulation of each of the procedures when the simulation is performed in the environment of Intel Core i7-3700K CPU @3.5GHz with 16.00 GB RAM and 64-bit Windows 7 Professional Operating System. As the procedures are simulated under the same conditions, the elapsed times presented in the table give an indication of the required computation volume of each procedure with respect to those of the others. It takes the shortest time to complete the adaptive clipping, which reflects the smallest computation volume among the four procedures, but has its weakness in image quality. As mentioned previously, each of the other three procedures is a combination of the CLAHE process and low-pass filters. Thus they need more computation with respect to that of CLAHE. Comparing the three procedures, those involving the proposed algorithms require much less time, i.e., computation volume, than that of the iterated TMR.

Table 4.3. Average elapsed time in second.

Input image	Image dimension	CLAHE	Iterated TMR filtering	Adaptive Clipping	Proposed algorithm 1	Proposed algorithm 2
X-ray	549*623	0.05	11.59	0.08	1.99	2.10
Window and desk	800*854	0.12	42.05	0.17	3.74	4.11
Pollen grain	512*672	0.10	20.85	0.15	2.01	2.16

#### **4.4. Summary**

In this chapter, the effectiveness of the two proposed algorithms has been evaluated

by the MATLAB simulation. The results have been examined by subjective observation and objective measurements. The algorithms have been compared with those produced by the iterated TMR filtering and adaptive clipping, two of the methods most relevant to this work. From the results, one can conclude that the two proposed algorithms lead to a good performance in high quality low noise contrast enhancement.

## Chapter 5. Conclusion

### *5.1. Concluding remarks*

The objective of the work presented in this thesis is to develop algorithms of the pixel classification for a cascaded low-pass filtering stages to remove noise generated in a HE process. The classification is expected to result in a number of masks, each of which protects a class of pixels located in the areas of a certain level of non-homogeneity. These masks are then used to achieve a high-quality low-noise enhancement. The quality of the LP filtering operations, in terms of noise removal and signal preservation, depends on the precision of the different levels of protection, which is related to the quality of the classification.

Signal gradients of the pixels in a region can be used to detect the gray level homogeneity. A HP filtering operation is applied to generate the signal gradients and their distributions are then obtained. In an image of good gradient condition, one can determine, by means of a simple analysis of the gradient distribution, multiple thresholds values to classify the pixels according to a given level of homogeneity. However, the gradient signals in most of the input images are degraded as image signal can be attenuated under different acquisition conditions. One cannot classify the pixels by a simple thresholding as the regional homogeneity in the input image is not simply related to the gradient amplitudes. Therefore, the pixels should first be grouped in such a way that the pixels in the same group are easily “distinguishable” by a simple gradient

thresholding so that a high-quality overall classification can be achieved by combining the classification results of the individual group. Two classification algorithms, each involving a different grouping, have been proposed.

The first algorithm aims at low contrast images acquired in HDR scenes, of which over-and-under exposure may seriously degrade the signal gradients during the acquisition process. As the gradient degradation in HDR images is often gray-level dependent, the gray-level range of the image is divided into sub-ranges, and the pixels in each sub-range make a group. In this way, the global gradient distribution is decomposed into the sub-distributions given by the pixel groups, making the gradient analysis performed in the sub-ranges and thus adapt to local gray level signals. The pixels of the same gradient are sorted and classified differently according to their gray level sub-range. Binary masks obtained in different pixel groups are combined to make final binary masks. In the case presented in this thesis, the image has been divided into three sub-ranges and nine binary masks have been generated. They have been combined to produce three controlling masks for the multi-stage LP filters.

The other algorithm has been proposed to tackle a pixel classification in a wider range of low-contrast images with different motives/textures in which signal gradients may be degraded due to various causes. To be more specific, it has been designed to identify a specific pixel class, e.g., those in non-homogeneous regions, from an image where the gradient degradation is not necessarily gray-level-dependent. In this algorithm, a gray level histogram thresholding has been performed to divide the pixels into two

groups according to the height of the gray level bins, i.e., their likelihood to be in homogeneous, or non-homogeneous, groups. In high-bin group, a majority of homogeneous pixels is against the minority of non-homogeneous ones. In the low-bin group, the situation is in the opposite direction. Such a pixel grouping differentiates the gradients of the minority pixels from those of the majority pixels. The gradient thresholding method can then be applied to identify the minority pixels. For the pixel grouping, the value of the gray level histogram threshold can be adjusted to pre-determine the concentration of the majority pixels in the subsequent pixel group. By applying different gray-level histogram thresholds, one can produce different masks for different levels of protection/exposure. To be more specific, the lowest histogram threshold value is applied to generate a controlling mask in order to distinguish the non-homogeneous pixel from the rest of the image for the protection, while another mask with the highest histogram threshold value aims at expose the homogeneous pixel and shields all the others.

In order to evaluate the effectiveness of the two algorithms, the contrast enhancement scheme involving the proposed algorithms has been applied, by MATLAB simulation, to three images from different sources. The results of the subjective observation and objective measurements have been obtained. They have been compared with those produced by two of the advanced contrast enhancement schemes most relevant to this work. One can see that the two proposed algorithms have led to a good performance in a high-quality low-noise contrast enhancement with less computation complexity.

## ***5.2. Future work***

In this thesis, two algorithms have been proposed to classify the pixels of an image of very poor contrast according to the homogeneity of their regions. Many efforts have been done in this work trying to achieve a high-quality and low-noise enhance, of which the effectiveness has been proven by the simulation results. As for the improvement of the proposed algorithms, there exist several possibilities for future work to optimize their performance.

One possibility is to further analyze and more systematically choose the thresholds used to group the pixels for the classification. In particular, the histogram thresholds used in the second algorithm can be defined in a more elaborate way. Besides using different percentage of the peak of the histogram as threshold values, one can also consider the influence of the valley and the slope in the gray-level histogram. Therefore, after pixel grouping, the majority pixels will have more concentration in the sub-group, resulting less possibility of misclassification of the minority ones.

Another extent can be achieved by optimizing the scheme of the classification, e.g., the process of gradient analysis and threshold generation. It is expected that CLAHE and the classification can be finished at the same time so that the LP filters do not need to wait for the completion of the classification. Such improvements can result in less processing time and more efficiency for the achievement of the algorithms in the MATLAB environment.

## References

- [1] J. Rabin, J. Delon, Y. Gousseau, "Removing Artefactes from Color and Contrast Modifications," *IEEE Transactions on Image Processing*, vol.20, no.11, pp.3073-3085, 2011.
- [2] M. D. Grossberg, S. K. Nayar, "Modeling the Space of Camera Response Functions," *IEEE Transactions on Pattern Analysis and Machine Intelligence*, vol.26, issue.10, pp.1272-1282, 2004.
- [3] J. Qin, M. R. El-Sakka, "A New Wavelet-based Method for Contrast/Edge Enhancement," *International Conference on Image Processing*, 2003, vol.2, pp. 397-340.
- [4] E. Lee, S. Kim, W. Kang, D. Seo, J. Paik, "Contrast Enhancement Using Dominant Brightness Level Analysis and Adaptive Intensity Transformation for Remote Sensing Images," *IEEE Geoscience and Remote Sensing Letters*, vol.10, no.1, pp.62-66, 2013.
- [5] T. Arici, S. Dikbas, Y. Altunbasak, "A Histogram Modification Framework and Its Application for Image Contrast Enhancement," *IEEE Transactions on Image Processing*, vol.18, no.9, pp.1921-1935, 2009.
- [6] A. Nieminen, P. Heinonen, Y. Neuvo, "A New Class of Detail-Preserving Filters for Image Processing," *IEEE Transactions on Pattern Analysis and Machine Intelligence*, vol.PAMI-9, no.1, pp.74-90, 1987.
- [7] N. Madhu, A. Spriet, S. Jansen, R. Koning, J. Wouters, "The Potential for Speech Intelligibility Improvement Using the Ideal Binary Mask and the Ideal Wiener Filter in Single Channel Noise Reduction Systems: Application to Auditory Prostheses," *IEEE Transactions on Audio Speech and Language Processing*, vol.21, no.1, pp.63-72, 2013.

- [8] Y. -T. Kim, "Contrast Enhancement Using Brightness Preserving Bi-histogram Equalization," *IEEE Transactions on Consumer Electronics*, vol.43, no.1, pp.1-8, 1997.
- [9] S. -D. Chen, A. Ramli, "Minimum Mean Brightness Error Bi-histogram Equalization in Contrast Enhancement," *IEEE Transactions on Consumer Electronics*, vol.49, no.4, pp.1310-1319, 2003.
- [10] C. H. Ooi, N. A. M. Isa, "Adaptive Contrast Enhancement Methods with Brightness Preserving," *IEEE Transactions on Consumer Electronics*, pp.2543-2551, 2010.
- [11] S. M. Pizer, E. P. Amburn, J. D. Austin, R. Cromartie, A. Geselowitz, T. Greer, B. T. H. Romeny, J. B. Zimmerman, K. Zuiderveld, "Adaptive Histogram Equalization and Its Variations," *Computer Vision, Graphics, and Image Processing*, vol.39, 1987, pp.355-368.t
- [12] Z. Xu, X. Liu, X. Chen, "Fog Removal from Video Sequences Using Contrast Limited Adaptive Histogram Equalization," *International Conference on Computational Intelligence and Software Engineering*, 2009.
- [13] R. C. Gonzalez, R. E. Woods, *Digital Image Processing*, 2<sup>nd</sup> Edition, Englewood Cliffs, NJ: Prentice Hall, 2002.
- [14] A. Buades, B. Coll, J. Morel, "A Review of Image Denoising Algorithms, with a New One," *Multiscale Modeling and Simulation*, vol.4, no.2, pp.490-530, 2005.
- [15] J. Astola, P. Heinonen, Y. Neuvo, "Linear Median Hybrid Filters," *IEEE Transactions on Circuits and Systems*, vol.36, no.11, pp.1430-1438, 1989.
- [16] C. Tomasi, R. Manduchi, "Bilateral Filtering for Fray and Color Images," *in International Conference on Computer Vision*, 1998.

- [17] L. Yaroslavsky, *Digital Picture Processing: An Introduction*, German: Springer-Verlag, 1985.
- [18] S. Chimire, H. Wang, "Classification of Image Pixels Based on Minimum Distance and Hypothesis Testing," *Computational Statistics and Data Analysis*, 2012.
- [19] Dutta S., Chaudhari B. B., "Homogeneous Region Based Color Image Segmentation," in *Proceedings of the World Congress on Engineering and Computer Science*, vol.2, 2009.
- [20] Coleman G., Andrews H., "Image Segmentation for Clustering," in *Proceedings of the IEEE* 67, 1979, pp.773-785.
- [21] Vicent L., Soille P., "Watersheds in Digital Spaces: an Efficient Algorithm Based on Immersion Simulation," *IEEE Transactions on Pattern Analysis and Machine Intelligence*, 1991.
- [22] S. E. Umbaugh, *Computer Imaging: Digital Image Analysis and Processing*, CRC Press, 2005.
- [23] Y. Zheng, J. Rao, L. Wu, "Edge Detection Methods in Digital Image Processing," in *the 5<sup>th</sup> International Conference on Computer Science & Education*, pp.471-473, Aug. 24-27, 2010.
- [24] P. Sahoo, S. Soltani, A. Wong, "A survey of Thresholding Techniques," *Computer Vision, Graphics, and Image Processing*, vol.41, no.2, pp.233-260, 1988.
- [25] J. Stark, "Adaptive Image Contrast Enhancement using Generalization of Histogram Equalization," *IEEE Transactions on Image Processing*, vol.9, no.5, pp.889-896, 2000.

- [26] Q. Wang, R. K. Ward, "Fast Image/Video Contrast Enhancement Based on Weighted Thresholded Histogram Equalization," *IEEE Transactions on Consumer Electronics*, pp.754-767, 2007.
- [27] M. Abdullah-Al-Wadud, Md. H. Kabir, M. A. A. Dewan, O. Chae, "A Dynamic Histogram Equalization for Image Contrast Enhancement," *IEEE Transactions on Consumer Electronics*, vol.53, issue 2, pp.593-600, 2007.
- [28] S. M. Pizer, R. E. Johnston, J. P. Ericksen, B. C. Yankaskas, K. E. Muller, "Contrast-Limited Adaptive Histogram Equalization: Speed and Effectiveness," in *Proceedings of the First Conference on Visualization in Biomedical Computing*, 1990, pp.337-345.
- [29] A. Boschetti, N. Adami, R. Leonardi, M. Okuda, "High Dynamic Range Image Tone Mapping Based on Local Histogram Equalization," *IEEE International Conference on Multimedia & Expo.*, 2010, pp.1130-1135.
- [30] Y. Gal, A. J. Mehnert, A. P. Bradley, K. McMahon, D. Kennedy, S. Crozier, "Denoising of Dynamic Contrast-Enhanced MR Images Using Dynamic Non-Local Means," *IEEE Transactions on Medical Imaging*, vol.29, no.2, pp.302-310, 2010.
- [31] B. Begovic, V. Stankovic, L. Stankovic, "Contrast Enhancement and Denoising of Poisson and Gaussian Mixture Noise for Solar Images," *18<sup>th</sup> IEEE International Conference on Image Processing*, 2011, pp.185-188.
- [32] S. Guillon, P. Baylou, M. Najim, "Robust Nonlinear Contrast Enhancement Filters," *International Conference on Image Processing*, 1996, pp.757-760.
- [33] N. Strobel, S. K. Mitra, "Quadratic Filters for Image Contrast Enhancement," *1994 Conference Record of the Twenty-Eighth Asilomar Conference on Signals, Systems and Computers*, 1994, pp.208-212.

- [34] J. -Y. Kim, L. -S. Kim, S. -H. Hwang, “ An Advanced Contrast Enhancement Using Partially Overlapped Sub-block Histogram Equalization,” *IEEE Transactions on Circuits and Systems for Video Technology*, vol.11, no.4, pp.475-484, 2001.
- [35] F. Lamberti, B. Montrucchio, A. Sanna, “CMBFHE: a Novel Contrast Enhancement Technique Based on Cascaded Multistep Binomial Filtering Histogram Equalization,” *IEEE Transactions on Consumer Electronics*, vol.52, no.3, pp.966-974, Aug. 2006.
- [36] C. Wang, B. Nahar, “Low-Pass Filtering Aiming at Noise Generation in a Contrast Enhancement,” *IEEE Midwest Symposium on Circuits and Systems, Ohio, USA*, Aug.2013.
- [37] X. Wang, G. Shi, Y. Niu, “Image Denoising Based on Improved Adaptive Directional Lifting Wavelet Transform,” *in ICSP 2008 Proceedings*, pp. 1112-1115.
- [38] T. -L. Ji, M. K. Sundareshan, H. Roehrig, “Adaptive Image Contrast Enhancement Based on Human Visual Properties,” *IEEE Transactions on Medical Imaging*, vol.13, no.4, pp.573-586, 1994.
- [39] N. R. Pal, S. K. Pal, “A Review on Image Segmentation Techniques,” *Pattern Recognition Society*, Pergamon Press Ltd., vol.26, no.9, pp.1277-1294, 1993.
- [40] William K. Pratt, *Digital Image Processing: PIKS Inside*, Third Edition, John Wiley & Sons, Inc.2001.

## Appendix

*Values of the parameters used in the simulation of TMR filtering method [3].*

Image	No. of iterations	Radius of disk, $W$	Intensity domain standard deviation, $\sigma$
X-ray	3	5	0.07
Window and Desk	3	10	0.04
Pollen Grain	3	10	0.05

*Values of the parameter used in the simulation of adaptive clipping method [4].*

Image	Linear dependence between $\alpha$ and the mean and variance, $a$
X-ray	0.02
Window and Desk	0.13
Pollen Grain	0.06